ISTANBUL TECHNICAL UNIVERSITY ★ GRADUATE SCHOOL OF SCIENCE ENGINEERING AND TECHNOLOGY

FLUTTER STABILIZATION OF LONG-SPAN BRIDGES BY MEANS OF WINGS AND IMPROVING THESE WINGS CONSIDERING CONVENTIONAL WING DESIGN

M.Sc. THESIS

Ibrahim KARLIDAG

Department of Civil Engineering

Structural Engineering Programme

NOVEMBER 2015

ISTANBUL TECHNICAL UNIVERSITY ★ GRADUATE SCHOOL OF SCIENCE ENGINEERING AND TECHNOLOGY

FLUTTER STABILIZATION OF LONG-SPAN BRIDGES BY MEANS OF WINGS AND IMPROVING THESE WINGS CONSIDERING CONVENTIONAL WING DESIGN

M.Sc. THESIS

Ibrahim KARLIDAG
(501111026)

Department of Civil Engineering

Structural Engineering Programme

Thesis Advisor: Assoc. Prof. Dr. Filiz PIROGLU

NOVEMBER 2015

İSTANBUL TEKNİK ÜNİVERSİTESİ ★ FEN BİLİMLERİ ENSTİTÜSÜ

KANATLAR VASITASIYLA UZUN ACIKLIKLI KÖPRÜLERİN ÇIRPINTI DENGELEMESİ VE BU KANATLARIN BİLİNEN KANAT TASARIMI UYARINCA GELİŞTİRİLMESİ

YÜKSEK LİSANS TEZİ

İbrahim KARLIDAĞ
(501111026)

İnşaat Mühendisliği Anabilim Dalı

Yapı Mühendisliği Programı

Tez Danışmanı: Doç.Dr. Filiz PİROGLU

KASIM 2015

Ibrahim Karlidag, a **M.Sc.** student of ITU **Graduate School of Science Engineering and Technology** student ID **501111026**, successfully defended the **thesis/dissertation** entitled "FLUTTER STABILIZATION OF LONG-SPAN BRIDGES BY MEANS OF WINGS AND IMPROVING THESE WINGS CONSIDERING CONVENTIONAL WING DESIGN" which he prepared after fulfilling the requirements specified in the associated legislations, before the jury whose signatures are below.

Thesis Advisor :	**Prof. Dr. Filiz PIROGLU** İstanbul Technical University	.....
Co-advisor :	**Prof.Dr. Uwe STAROSSEK** Hamburg Technical University	.....
Jury Members :	**Yrd.Doc.Dr. Nilgun AKTAN** Yıldız Technical University	.....
	Yrd. Doc.Dr. Kadir OZAKGUL İstanbul Technical University	.....

Date of Submission : 18 November 2015
Date of Defense : 30 December 2015

To my family, friends and especially to precious Topal family,

FOREWORD

This thesis is made as a master project, as part of the requirements for the awarding of a degree in Master of Science in Engineering at the department of Structural Engineering at the Technical University of Istanbul (ITU) and the Technical University of Hamburg-Harburg (TUHH).
I would like to express my sincere gratitude to my leading supervisor Assoc. Prof. Dr. Filiz PIROGLU for all his valuable discussions and support. Further I would like to thank my co-supervisor Prof. Dr.-Ing. Uwe Starossek for his great co-operation and help.
Finally, I wish to express my gratitude to friends and Topal family for their supports during the study of this work. .

November 2015

Ibrahim KARLIDAG
(Civil Engineer)

TABLE OF CONTENTS

Sayfa

ABBREVIATIONS

b	**:** Half of the plate width
B	**:** Typical chord or deck width dimension
c	**:** Damping coefficient of the structure
$\boldsymbol{\alpha}$	: (i) Effective angle of attack (ii) Torsional displacements of the structure
$\mathbf{D_\alpha}$	**:** Aerodynamic drag force
$\mathbf{C_D}$	**:** Drag force coefficient
$\mathbf{C_L}$	**:** Lift force coefficient
$\mathbf{C_M}$	**:** Moment coefficient
D	**:** Cylinder diameter
ρ	**:** Air density
b	**:** Half of the plate width
NACA	: National Advisory Committee for Aeronautics
EC 3	**:** Eurocode 1993-1
SAP 2000	**:** Integrated Software for Structural Analysis And Design

LIST OF TABLES

Page

LIST OF FIGURES

Page

FLATTER STABILIZATION OF LONG-SPAN BRIDGES BY MEANS OF WINGS AND IMPROVING THESE WINGS CONSIDERING CONVENTIONAL WING DESIGN

SUMMARY

It is obvious fact that the cable-supported bridges, including both cablestayed bridges and suspension bridges, are choosen more day by day around the world because of their sufficiency for long spans. Even though they let the engineers to span long distances, this type of long span birdges are known generally remarkably flexible, in terms of damping is low efficient and in the sense of weight is light. Thus, these long-span cable supported bridges can also be susceptible to wind effects. The oscilation of the long-span bridges and aerodynamic stability of cable-stayed bridges are one of the major concern in bridge engineering. For example, the Tacoma Narrows suspension bridge, which had a main span of 853m and was built to link the Olympic Peninsula with the rest of the state of Washington, oscillated through large displacements at a wind speed of about 19 m/s and collapsed on November 7, 1940, only four months and six days after the bridge was opened to the public.

As compared to other types of bridges, long-span cable-supported bridges are remarkably flexible. Since cable-stayed bridges are extremely slender, unexpected results of the wing effects on these bridges and aerodynamic problems in cable-supported bridges led engineers to concern about wind effects. Although cable-stayed bridges have been found surprisingly stable aerodynamically, several bridges have required special improvement against wind action on bridges.

The different engineering branches have in common to improve engineering problems through their perspective and people from around the world labor to contribute technical progress in their related field. Not only in the scientific field, but also in practice, research to optimize issues and to figure out the new solutions to relevant questions.

Due to its delicate construction, suspension bridges brings specific problems with the need to be considered already in the design. One of these problems is the wind generated flutter, a problem of stability for the suspension bridges is particularly vulnerable. A wind load is a highly unsteady operation. At the critical wind speed known as the air forces act in resonance with the bridge and lead to the steady growth of the amplitudes. This swings the bridge with the flutter natural frequency, which is always located between the rotational natural frequency and the natural bending frequency. Flutter occurs only when the rotational natural frequency is above the natural frequency of the bending vibration. At very low and very high frequency ratios flapping is prevented or impeded.

In the previous studies, it was found found ways to stabilaze this oscillation such as increasing the rotational stiffness and forming the deck shape as aerodynamic body. An increase in the difference between the first bending frequency and the first rotational natural frequency has a favorable effect on the critical wind speed. Improving the deck section from conventional form to the aerodynamic shape is one of these studies which was carried out in practical field.

This new method has been already studied and the necessary prior arrangments has been identified in former master subject. The former subject was investigated to increase the flutter resistance of long-span bridges. The resulting air forces there are means of one or both sides attached wing structure contributing to raising the critical wind speed of the overall system. The wings were only intended to contribute to stability and flutter not participating in the load transfer. They were not used as a roadway or sidewalk, but should be able to be manufactured and installed as low as possible. Furthermore, they should have been as light as possible and not interfere with the overall aesthetics of the bridge.

In this work, considering these ideas and the knowledge which mentioned above, it has been intended to improve the attached wing structures from the previous plate-like wing structure to symmetric elliptic airfoil sectioned wing structure by using conventional wing design.

KANATLAR VASITASIYLA UZUN AÇIKLIKLI KÖPRÜLERİN ÇIRPINTI DENGELEMESİ VE BU KANATLARIN BİLİNEN KANAT TASARIMI UYARINCA GELİŞTİRILMESİ

ÖZET

Kablo askılı köprüler ve asma köprülerin içinde bulunduğu kablo destekli köprüler, uzun açıklıklardaki yeterlilikleri sayesinde dünya çapında oldukça fazla tercih edildikleri açık bir gerçektir. Bu köprü türünün mühendislere uzun açıklıkları aşma imkân vermesine rağmen, bu uzun açıklıklı köprüler genellikle önemli derecede esnek, sönümleme açısından düşük ve ağırlık yönünden ise hafiftir. Bu özelliklerinden dolayı uzun açıklıklı kablo destekli köprüler rüzgar etkilerine karşı oldukça duyarlı olabiliyorlar.

Uzun açıklıklı köprülerin titreşimleri ve kablo askılı köprülerin aerodinamik stabilitesi köprü mühendisliği alanında mühendislerin en büyük sorunlarindan biridir. Örnek olarak, 853 metre ana açıklığa sahip ve Olimpic Yarimada ile Washington eyaletinin kalan kısmı arasında bağlantı olarak inşaa edilen Tacoma Narrows asma köprüsü, 19 m/sn'lik bir rüzgar hızındaki büyük yerdeğistirmeler ile salındı ve kamuya açılışından dört ay altı gün sonar 1940 yılı Kasim 7'de yıkıldı.

Diğer köprü türleri ile karşılaştırıldığında, uzun açıklıklı kablo destekli köprüler önemli ölçüde esnektir. Kablo askılı köprüler son derece narin oldukarı için, köprü üzerindeki beklenmeyen rüzgar etkileri ve aerodinamik sorunlar mühendisleri rüzgar etkileri üzerine düşünmeye sevketmistir.

Kablo askılı köprülerin şaşırtıcı şekilde aerodinamik açıdan istikrarlı olmalarına rağmen, çoğu köprüler rüzgar etkilerine karşı bazı özel iyileştirmeler gerektirmişlerdir. Bu iyileştirmeler bazen köprü tabliyesinin kendi şekli ile çözülmeye çalışılmış, bazende ek elemanlar veya aygıtlar ile sağlanmaya çalışılmıştır. Bunlara örnek olarak pasif ve aktif sönümleyiciler günümüzde verilebilecek en yaygın örneklerdir. Fakat bu ilave sönümleyicilerin yanında köprünün rüzgâr dayanımını arttıracak daha ekonomik ve uygulanabilirliği yüksek farklı düşünceler mühendislerce ve tasarımcılarca halâ denenmekte ve araştırılmaktadır.

Her mühendislik branşının ortak yönü, mesleki alandaki problemlerinin çözümlerini hem kendi perspektiflerinden bakarak geliştirmeleri hem de dünyanın dört bir tarafında süregelen çalışmaların mühendislik teknik birikimine katkıda bulunmasıdır. Mühendisliği bilimsel alanda icra eden akademisyen camia kadar, uygulamada görev alan çevre de, mesleki sorunlara optimize çözümler getirmek ve yeni çözüm teknikleri geliştirmek amacıyla araştırmalar yapmaktadır. Bu araştırmaların sonuçları ve kattığı yeni bilgiler diğer alanlarda da kullanılarak optimize sonuçlar elde edilmeye çalışılmaktadır.

Bu tez yapı mühendisliği kapsamında yazılıyorsa da, yukarıda belirtilen bilgiden dolayı uçak mühendisliği kapsamındaki görüşlerden faydalanılarak ve bu bilgileri yapı mühendisliği kapsamında uygulayarak farklı perspetiflerin birleştirilmesi öngörülmüştür.

Kanatların tasarımında aeroelastisite ve aerodinamik etkiler göz önünde bulunudurularak kanatlara etkiyen rüzgar yükleri ve bunların ek etkileri hesaplanmaya çalışılmıştır. Rüzgar yüklerinin hesabı yapı mühendisliğinde biliniyorsada kanatın kesitinden ve yapısından dolayı daha narin ve detaylı hesaplar gerekmiştir. Bu detaylı hesapların yapılabilmesi ve ilgili katsayıların hesaplanabilmesi için uçak mühendisliğinde yaygın olarak kullanılan ticari bilgisayar programlarından yararlanılmış ve bu değerler amprik formüllerin sonuçları ile kontrol edilmiştir.

Asma köprü inşaatlarının büyük hassasiyet gerektirmesi dolayısıyla, ortaya tasarım aşamasında göz önüne alınması gereken belli başlı problemler çıkmaktadır. Bu sorunlardan birisi de rüzgarın çırpınma etkisidir ki bu problem asma köprüleri stabilite açısından savumasız hale getirmektedir. Rüzgar yükü çok değişken bir parametrik özelliktedir. Hava akımının köprü ile aynı rezonansta hareket etmesi durumunda ortaya çıkan kritik rüzgar hızında, genlikler sürekli olarak büyümekte ve. bu durum da köprüyü çırpınma doğal titreşim frekansında sallamaktadır. Bu frekans, her zaman dönme doğal titreşim frekansı ve eğilme doğal titreşim frekansının arasında yer alır. Çırpınma, yalnızca dönme doğal titreşim frekansı, eğilme doğal tireşim frekansından daha yüksek değerde ise gerçekleşir. Çok düşük ve çok yüksek frekans değerlerinde çırpınma etkisi önlemiş veya zorlaştırılmıştır.

Önceki çalışmalarda bu salınımı stabilize etmek, için dönme rijitliğini artırmak ve tabliyenin geometrisini aerodinamik bir biçime getirmek gibi çözümler üretilmiştir. Birinci doğal eğilme frekansı ve birinci doğal dönme frekansı arasındaki farkı artırmak da, kritik rüzgar hızında istenen olumlu etkiyi yaratmıştır. Bu araştırmalardan birinde geliştirilen, tabliye kesitini geleneksel formundan, aerodinamik forma çevirmek yönündeki bir çözüm ise uygulama alınına da taşınmıştır.

Bu yeni teknik üzerine çalışmalar yapılmış ve gerekli başlangıç düzenlemeleri daha önceki yüksek lisans tez çalışması kapsamında belirlenmiştir. Önceki çalışma, büyük açıklık geçen köprülerin çırpınma dayanımını artırmak amacını taşımaktadır. Hava kuvvetlerinin bileşkesi, tüm sistemin kritik rüzgar hızını artırmaya katkıda bulunan, bir veya iki taraftaki kanatlara karşılanır. Kanatlar sadece stabiliteye katkıda bulunmak ve çırpınma etkisini azaltmak amacıyla yerleştirilirler; yük aktarımı sağlama amacı yoktur. Kanatlar ayrıca; araç veya insan yürüme alanı olarak kullanılmaz; mümkün olduğunca hafif konstrüksiyondan teşkil edilmelidir. Ayrıca; köprünün estetik bütünlüğünü bozmayacak biçimde tasarlanmalıdır.

Bu araştırma kapsamında tasarlanan kanatlar plaka olarak tasarlandığından ve bu plakaların aralıkları 2 m olduğundan dolayı uygulanabilirliği çok yüksek değildir. Uygunlanabilirliği etkileyen ağırlık ise diğer bir problemdir. Bu problemleri ortadan kaldırmak ve kanatların köprülerde ki uygulanabilirliğini ve verimini arttırmak amacıyla yeni bir tasarım düşünülmüştür.

Yukarda belirtilen düşünce ve bilgilerin ışığında tabliyeye eklenen kanat yapılarının tasarımlarında bu kanatların ekonomikliği ve ağırlıkları göz önünde bulundurularak daha önceki plaka benzeri geometri yerine, geleneksel kanat tasarımı ile teşkil edilen simetrik eliptik uçak kanadı biçimi tercih edilmiş ve ileri seviyede iyileştirilme yapılması hedeflenmiştir.

Bu tez kapsamında düşünülen geleneksel kanat tasarımı için kanat kesiti rüzgarı iki farklı taraftan karşılaması amacıyla eliptik ve simetrik olarak karar verilmiş ve tek bir kanatın uzunluğu eski kanatın uzunluğu olan 2 m'den 20 m'ye değiştirilerek hem destek elemanlarının sayısı azaltılıp hemde daha uygulanabilir sonuçlar elde edilmeye çalışılmıştır.

Kanatların rüzgar etkileri ve kanatların ağırlıkalrı belirlendikten sonar inşaat mühendisliği kapsamında kanatları köprüye bağlayan destekler tasarlanmış ve bunlarda da hafiflik ve iyileştirilmeye gidilmiştir. Desteklerin kafes system olarak seçilmesi ekonomiklik açısından tercih edilmiştir.

1. INTRODUCTION

The development of modern materials and construction techniques has resulted in a new generation of lightweight flexible structures. Such structures are usually susceptible to the action of winds. Suspension bridges and cable-stayed bridges are typical structures susceptible to wind-induced problems.

The most renowned bridge collapse because of winds is the Tacoma Narrows suspension bridge linking the Olympic Peninsula with the rest of the state of Washington. It was completed and opened to traffic on July 1, 1940. Its 853 m (2799 ft) main suspension span was the third longest in the world. This bridge became famous for its serious wind-induced problems that began to occur soon after it opened. On November 7, 1940, four months and six days after the bridge was opened, the deck oscillated through large displacements in the vertical vibration modes at a wind velocity of about 68 km/h. The motion changed to a torsional mode about 45 minutes later. Finally, some key structural members became overstressed, and the main span collapsed.

Some bridges were destroyed by wind action before the failure of the Tacoma Narrows Bridge. However, it was this failure that shocked and intrigued bridge engineers to conduct scientific investigations of bridge aerodynamics. Some existing bridges, such as the Golden Gate suspension bridge in California with a main span of 1280 m (4200 ft), also experienced large wind-induced oscillations, though not to the point of collapse. In 1953, the Golden Gate Bridge was stiffened against aerodynamic action (Cai, 1993) [1].

1.1 Purpose of Thesis

The present work is concerned with the increase in the critical wind velocity for the flutter of suspension bridges with symmetric elliptical airfoil cross-section by means of a wing structure, aims to examine the wing structure a real or fictional bridge and serve as a basis for calculation. It is believed to be a useful substitute system which can be used and to improve the further steps for the previous parametric study.

Subject of study parameters have been obtained from previous study. These parameters can differ for vane assemblies in the longitudinal direction. The influence of leaf width and spacing of the blades to the bridge axis at the critical wind speed have been also obtained from previous study in order to improve the shape of the wing structure and the critical wind speed.

The previous work was concerned with the increase in the critical wind velocity coming fluttering of suspension bridges with plate-like cross-section by means of same way. The results of the parametric study have been presented by means of closed formulas developed in previous thesis which is called "Flatterstabilisierung von Brücken mittels starrer Flügel". Then a wing structure had been designed, sized and finally had been assessed to their costs. The proposed design may significantly raise the critical wind speed of the system.

Even though there are other approaches in order to reduce long span bridge's swinging, using wings was choosen for finding a cost-efficient, practicable and applicable design for bridge decks.

However, the former study was not applicable and cost-efficiency. Therefore in this study, longer, lighter and conventional wind design have been considered in order to make this fictional idea more realistic and practicable as well as innovative.

1.2 Literature Review

In this thesis, primarily aeroelasticity and the wind effects on bridges in literature are studied, and then some information about airfoil are given in more detail.

Wing geometry and the air flow around the airfoil are crucial in terms of the efficiency of the wind turbines. In this prospect, in the course of numerical analyses, a symmetric elliptical airfoil used. These analyses have been implemented in this research for a certain range of angle of attack and 59,6 m/sn wind speeds. The purpose here is to determine the effects of these parameters on the wing. The numerical solutions were carried out by using XLFR5 commercial software.

By using the datas related to the wind forces on the airfoil intended to design wing structure elements and the thickness of the members.

After determining the structural geometry of the wing, support reactions and the weigth of the wing have been used in order to design the support structures.

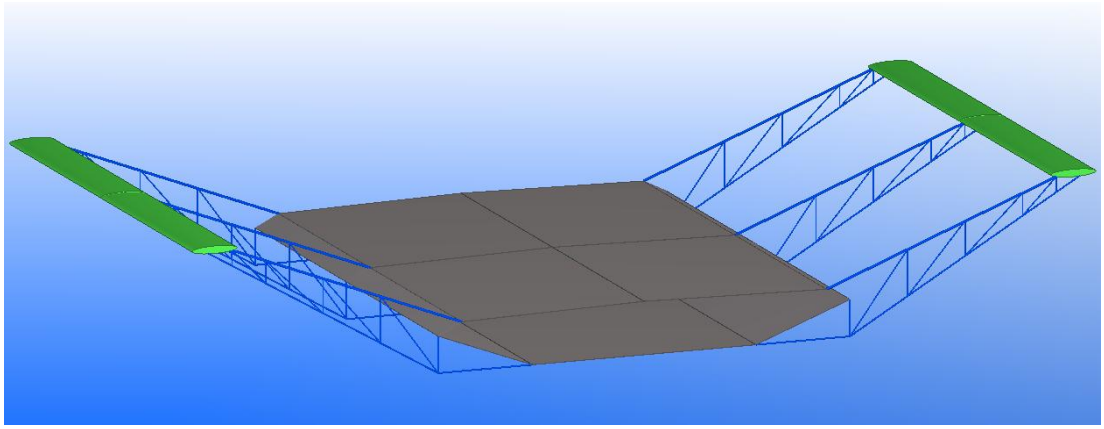

Figure 1.1 : 2-D structures for flutter analysis.

1.3 Hypothesis

In this study, it was purposed to increase the stability of the long span bridges by means of additional wings along the deck in the both sides which contribute to raise the critical wind speed against the fluttering. The subject of this thesis had been already intented to improve and upgrade the efficiency of the additional wing idea to the bridge deck with plate-like cross-section.

Adding wing structures to the bridge deck, along the whole bridge on both sides is thought to be a new approchment to stabilize the long span bridge oscilations. Active and passive systems are known the most common ways for stabilization of long span bridges and this new approachment is thought to be an innovative alternative to the other ones.

2. WIND EFFECTS ON LONG SPAN BIRDGES

2.1 Introduction

The development of modern materials and construction techniques has resulted in a new generation of lightweight flexible structures. Such structures are usually susceptible to the action of winds. Suspension bridges and cable-stayed bridges are typical structures more susceptible to wind-induced problems than the convebtional bridges.

The most renowned bridge collapse because of winds is the Tacoma Narrows suspension bridge linking the Olympic Peninsula with the rest of the state of Washington. It was completed and opened to traffic on July 1, 1940. Its 853 m (2799 ft) main suspension span was the third longest in the world. This bridge became famous for its serious wind-induced problems that began to occur soon after it opened. On November 7, 1940, four months and six days after the bridge was opened, the deck oscillated through large displacements in the vertical vibration modes at a wind velocity of about 68 km/h. The motion changed to a torsional mode about 45 minutes later. Finally, some key structural members became overstressed and the main span collapsed.

Some bridges were destroyed by wind action before the failure of the Tacoma Narrows Bridge. However, it was this failure that shocked and intrigued bridge engineers to conduct scientific investigations of bridge aerodynamics. Some existing bridges, such as the Golden Gate suspension bridge in California with a main span of 1280 m (4200 ft), also experienced large wind-induced oscillations, though not to the point of collapse. In 1953, the Golden Gate Bridge was stiffened against aerodynamic action (Cai, 1993) [1].

2.2 Long-Span Bridge Responses to Wind

Wind may induce instability and excessive vibration in long-span bridges. Instability is the onset of an infinite displacement granted by a linear solution technique.

Actually, displacement is limited by structural nonlinearities. Vibration is a cyclic movement induced by dynamic effects. Since both instability and vibration failures in reality occur at finite displacement, it is often hard to judge whether a structure failed due to instability or excessive vibration-induced fatigue damage to some key elements.

Instability caused by the interaction between moving air and a structure is termed either aeroelastic or aerodynamic instability. The term aeroelastic emphasizes the behavior of deformed bodies, where aerodynamic reflects the vibration of rigid bodies. Since many problems involve both deformation and vibration, these two terms are used interchangeably hereafter. Aerodynamic instabilities of bridges include divergence, galloping, and flutter. Typical wind-induced vibrations consist of vortex shedding and buffeting. These types of instability and vibration may occur alone or in combination. For example, a structure must experience vibration to some extent before flutter instability starts.

The interaction between the bridge vibration and wind results in two kinds of forces: motiondependent and motion-independent. The former vanishes if the structures are rigidly fixed. The latter, being purely dependent on the wind characteristics and section geometry, exists whether or not the bridge is moving. The aerodynamic equation of motion is expressed in the following general form:

$$[M]\{\ddot{Y}\} + [C]\{\dot{Y}\} + [K]\{Y\} = \{F(Y)\}_{md} + \{F\}_{mi} \qquad \textbf{(1.1)}$$

where [M] = mass matrix; [C] = damping matrix; [K] = stiffness matrix; {Y} = displacement vector; $\{F(Y)\}_{md}$= motion-dependent aerodynamic force vector; and $\{F\}_{mi}$= motion-independent wind force vector.

The motion-dependent force causes aerodynamic instability, where the motion-independent part together with the motion-dependent part causes deformation. The difference between short-span and long-span bridge lies in the motion-dependent part. For the short-span bridges, the motion-dependent part is insignificant and there is no concern about aerodynamic instability. For flexible structures like long-span bridges, however, both instability and vibration need to be carefully investigated [1].

2.3 Wind Loading in EN 1991-1-4

Wind loads on structures, such as buildings, bridges, masts, but also on parts of these structures, are derived from wind loading standards. Structural engineers within Europe will soon be obliged to use the Eurocode standart for the calculation of structures. Wind loads are given within this system in EN 1991, Actions on Structures, Part 1-4, Wind Loads. This code covers a wide range of building shapes and dimensions. However, many cases still exist for which the code gives no, or a very unsatisfactory, answer. For such cases, wind tunnel experiments, or in special cases, full scale experiments may lead to an answer for the behaviour.

In 1975, the Commission of the European Community decided on an action programme in the field of construction. The objective of the programme was the elimination of technical obstacles to trade and the harmonisation of technical specifications. In 2010, in all CEN countries, all national standards on the design of building structures will be replaced by the Eurocodes. All Eurocodes, however, include a National Annex, to specify values for which the Eurocode leaves national choice open. Without National Annex, and without translation in the official language of the country considered, the EN's can not be used widely and effectively.

The Eurocode standart is based on performance based design. This means that the action effects and the resistance of a structure are treated separately. Action effects are independent of structural material, unless the material itself is a source for an effect (e.g. temperature effects). The effects determine the level of the strength (performance) that needs to be fulfilled by the structure. The Eurocode series consists of 10 series of documents: EN 1990 to EN 1999, where EN 1991 deals with the actions.

EN 1991 ' Actions on Structure' specifies the haracteristic values of the actions on structures. EN 1991 is divided in 10 volumes, each specifying a specific action. The

wind loading is specified in EN 1991-1-4. [2].

2.4 Wind Actions on Bridges

There are a large number of limitations in order to use Eurocode1 for determining the effect of winds acting on bridges which some are as follows:

- The bridge must be first assessed that it is responding statically against the fluctuating wind load.

- If it is assessed that the bridge is acting dynamically against the fluctuating wind loads then the procedures given in the annex B and C may not be useful. This is due to the fact that the structural factors which account for the dynamic behavior of the structure are obtained based on the dynamic response component which is valid only for the response of building structures in the first cantilever mode, and it is not applicable to bridges or to many of the individual building structures which can even be regarded as being static.

- The methods recommended in chapter 8 of EC1 are valid only for the structures with mode shapes of constant sign or having simple linear mode shapes (cantilever structures), and it is not appropriate to use for continuous bridges, guyed masts, cable stayed or arch bridges.

- The method is covering only the response of the structure in the along-wind direction of the wind.

- The maximum height of the structure is 200, meter and the same is for the length of main span.

- The cross section and the depth of the bridge deck should be uniform

throughout the span of the bridge.

3. WIND-INDUCED VIBRATION AND ARODYNAMIC INSTABILITY

3.1 Introduction

Besides mean wind load and aerostatic instability, there are several mechanisms, related various wind speed ranges, that can excite dynamic response and aerodynamic instability of long-span cable-supported bridges. Wind-induced vibration is an important source of loads on bridge structures, whereas wind-induced aerodynamic instability is very dangerous to bridge structures and may cause the bridge to collapse.

Four types of wind-induced vibration and aerodynamic instability problems that all need to be considered in the design of a long-span cable-supported bridgeare as follows: [**2**].

- Vortex shedding excitation usually occurs at low wind speeds and low turbulence conditions, but it can cause considerable vibration of the bridge deck. The interaction of the bridge with vortex flow may result in the so-called “lock-in” phenomenon that leads to excessive bridge vibration. Vortex induced response of the bridge should be controlled to a certain limit in order to ensure normal operation under service loads/traffic loads and additionaly to avoid fatigue damage to the bridge.

- Galloping instability is caused by self-excited forces, and it occurs in vertical modes of the bridge deck. Galloping happens when the bridge deck continuously absorbs energy from the incoming wind flow and the vibration becomes divergent. It happens abruptly and can cause the bridge to collapse, so it should be stricktly avoided in the design of the bridge.

- Flutter instabilities of several types occur at very high wind speeds for bridge decks, as a result of self-excited aerodynamic forces. Flutter always involves

torsional motions and may also involve vertical bending motions, and it should be avoided in the design of bridges. It was flutter that caused the collapse of the original Tacoma Narrows Bridge in 1940.

- Buffeting excitation is caused by fluctuating forces induced by turbulence. It occurs over a wide range of wind speeds and normally increases monotonically with increasing wind speed. Excessive buffeting may cause fatigue damage problems in bridge components and affect functionality of the bridge. The buffeting should be considered in the design stage. [**2**]

3.2 Fluttering

Flutter is a self-feeding and potentially destructive vibration to a long-span cable-supported bridge where aerodynamic forces on the bridge deck couple with its motion. If the energy input of the aerodynamic forces under the cyclic motion of the strong winds in a cycle is larger than that the dissipated energy by the damping of the bridge structure system, the amplitude of the vibration of the bridge deck will increase. This increasing vibration will then amplify the aerodynamic forces, resulting in self-excited forces and self-exciting oscillations. The vibration amplitude of the bridge deck can build up until it results in the collapse of the bridge. One famous example of flutter phenomena was the collapse of the original Tacoma Narrows Bridge in 1940.

The term of classical flutter is originally applied to thin airfoils in the aircraft industry. It means an aeroelastic phenomenon in which two degrees of freedom (DOFs) of a structure, torsional and vertical, coupled together in a flow-driven, unstable oscillation. It is also called 2-D flutter. Single degree of freedom (1-D) flutter may manifest itself in a vertical or torsional mode of vibration of a structure, but torsional action is more serious by far. The celebrated failure of the original Tacoma Narrows Bridge exhibited two forms of 1-D flutter – initially a non-catastrophic vertical flutter and then, at a higher wind speed, a large-amplitude of torsional flutter. For modern long-span cable-supported bridges, flutter instability may involve multiple modes of vibration. [2]

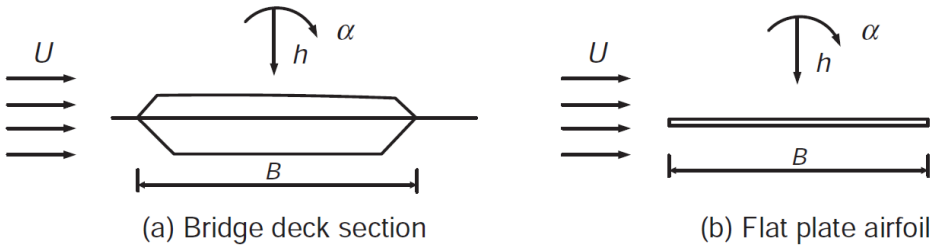

Figure 3.1 : 2-D structures for flutter analysis.

3.3 Buffeting

The aero-elastic phenomenon buffeting falls in the category of wind-induced vibrations caused due to wind turbulence that are created by the fluctuating and inconsistent forces. The velocity of the incoming wind is fluctuating in nature and hence results in an inconsistent force on the structure. When the pressure variations in the incoming wind force have a frequency similar to one of the natural frequencies of the bridge, resonance will occur. The response of the bridge to buffeting will mainly depend on the turbulence intensity, the natural frequencies and the shape of the structure. Buffeting along with flutter can cause large aerodynamic instabilities in long span bridges due to the large amplitude vibrations induced by them. [4].

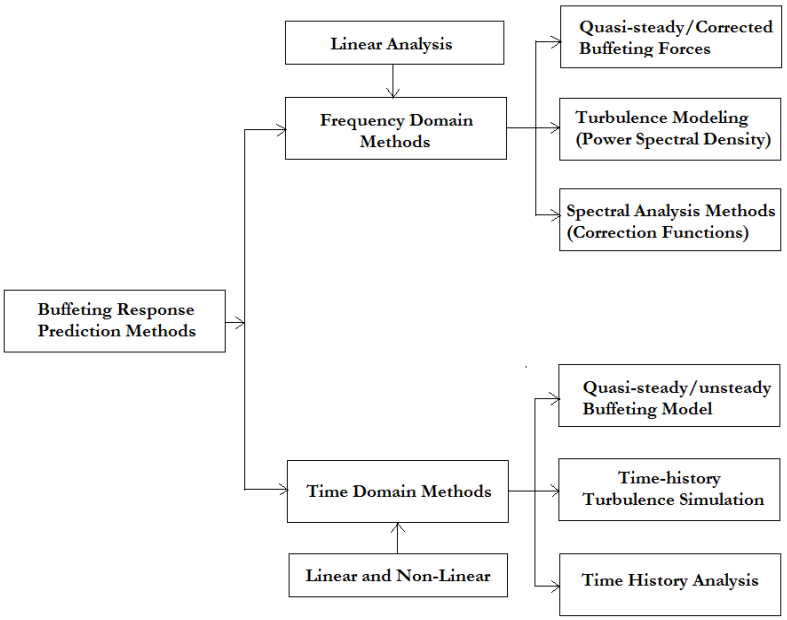

Figure 3.2: Buffeting response prediction classification.

Buffeting in bridges may cause serviceability discomfort due to high and unpredicted displacements and also cause fatigue failure of structural members of the bridge. Buffeting in structures can be a serious threat because it can be caused at variable

levels of fluctuating velocities and thus had the potential to cause serious damage to a structure. Buffeting can also take place in a coupled condition with flutter at high velocity ranges. The buffeting response analysis can be evaluated by the following two analytical approaches:

2. Frequency-domain approach (Linear behavior) or
3. Time-domain approach (Linear and non-linear behavior)

3.3.1 Frequency-domain approach

The frequency-domain analysis of buffeting response has been used during the recent times due to the fact that the time-domain analysis is time-consuming. In the frequency-domain, a Fourier transform is needed to apply in order togetforces from the time-domain to the frequency-domain with spectral analysis and statistical computation. Also, nDOF systems have been decomposed to single DOF using modal analysis technique. Geometrical and aerodynamic nonlinearity can be taken into account in the time-domain analysis.

3.3.2 Assumptions and uncertainties

In the time-domain approach, the wind forces are applied at discrete nodes of the structure. Both quasi-steady sectional forces (aerodynamic admittance) and unsteady forces (indicial functions) can be used in the time-domain models. At higher wind velocities causing coupled flutter and buffeting, the frequency-domain forces can be transformed into the time-domain forms using rational function approximation with frequency response function (FRF). Newmark and Wilson's direct integration methods can also be applied for the time-domain analysis for wind-structure interaction and corresponding responses.

3.3.3 Time-domain approach

Both the frequency-domain and the time-domain approaches are based on certain assumptions for simplifications specified by Le Thai Hoa as stated below:

1. Gaussian stationary processes assumptions: The fluctuating wind loads and velocities are treated as Gaussian stationary random processes.

2. Quasi-steady assumption: The unsteady buffeting forces are modeled as quasisteady buffeting forces by approximations made in the relative velocity and the

unsteady force coefficients. The relative velocity simplifed by omitting the unimportant components and force coefficients are linearly approximated from the Taylor series expansion.

3. Strip assumption: Line-like structures are divided into span-wise strips, and the unsteady forces on a single strip are caused by the forces acting only on that strip. At the same time, the forces acting on a single strip can be used to represent the entire line-like structure.

4. Correlation functions and transfer functions: Certain correlation functions such as aerodynamic admittance, coherence and joint acceptance, and transfer function such as mechanical admittance are added in transformation of statistical computation and single DOF input-output relation.

5. Modal uncoupling assumption: Multi-modal response is validated from generalized response. This assumption can be validated by the fact that the modal frequencies are diverse enough to create modal coupling and due to the complicated mechanism of the dynamic coupling of the modes.

3.3.4 Effects of buffeting on bridges

The buffeting phenomena can cause serious damages to bridges of which some are listed as follows:

- Serviceability discomfort.
- Fatigue damage to structural components.
- Structural failure when coupled with flutter at higher velocities resulting in structural collapse.

For the analytical approach of buffeting, Davenport proposed the quasi-static method by introducing the aerodynamic admittance function for considering the unsteady nature of the wind effects. The complex nature of various bridge crosssections was taken into account by Scanlan, where he suggested the aerodynamic coefficients be derived by the wind tunnel tests which are used to compute the self-excited force. Scanlan has also provided a relation between the aerodynamic admittance functions and the aerodynamic derivatives which forms the foundation of the conventional analysis procedure for buffeting [4].

The frequency domain approach for buffeting analysis is limited to linear structures without aerodynamic nonlinearities ignoring the aerodynamic coupling of modes. This is a major limitation as this method cannot be performed under ultimate strength conditions but only for serviceability checks. The buffeting force can be expressed in the form of matrix as follows:

$$\begin{Bmatrix} L_b \\ D_b \\ M_b \end{Bmatrix} = \frac{1}{2}\rho U^2 B \begin{bmatrix} 2C_L & \left(\frac{dC_L}{d\alpha} + C_D\right) \\ 2C_D & \frac{dC_D}{d\alpha} \\ 2C_M B & \frac{dC_M}{d\alpha} B \end{bmatrix} \begin{Bmatrix} \frac{u(t)}{\overline{U}} \\ \frac{w(t)}{\overline{U}} \end{Bmatrix} = \overline{U}^2 [C_b]\{\eta\} \quad \textbf{(3.1)}$$

where, C_L , C_D and C_M are the coeffcients for lift, drag and moment respectively, α is the angle of attack of wind, $[C_b]$ is the static coefficient matrix, and η is the turbulent wind component vector. [2]

3.4 Vortex Shedding

Vortex shedding is a wake-induced effect occurring on bluff bodies such as bridge decks and pylons. Wind flowing against a bluff body forms a stream of alternating vortices called a von Karman vortex street shown in Figure 3.3a. Alternating shedding of vortices creates an alternative force in a direction normal to the wind flow. This alternative force induces vibration. The shedding frequency of vortices from one surface, in either torsion or lift, can be described in terms of a nondimensional Strouhal number, S, as

$$S = \frac{ND}{\tilde{U}} \quad \textbf{(3.2)}$$

where N = shedding frequency and D = characteristic dimension such as the diameter of a circular section or depth of a deck.

The Strouhal number (ranging from 0.05 to 0.2 for bridge decks) is a constant for a given section geometry and detail. Therefore, the shedding frequency (N) increases with the wind velocity to maintain a constant Strouhal value (S). The bridge vibrates strongly but self-limited when the frequency of vortex shedding is close to one of the natural frequencies of a bridge, say, N 1 as shown in Figure 3.3b. This phenomenon is called lock-in and the corresponding wind velocity is called critical velocity of vortex shedding. [1].

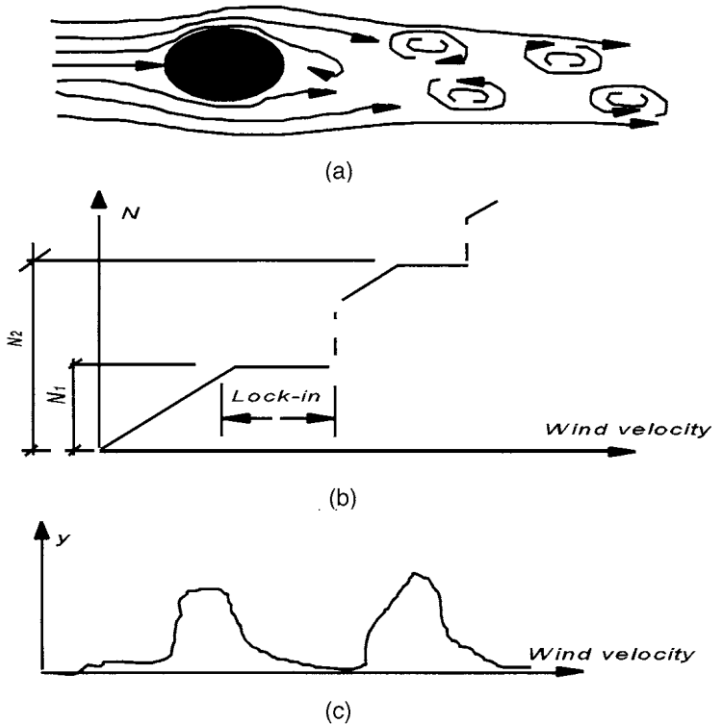

Figure 3.3: Explanation of vortex shedding. (a) Von Karman Street; (b) lock-in phenomenon; (c) bridge vibration.

The lock-in occurs over a small range of wind velocity within which the Strouhal relation is violated since the increasing wind velocity and a fixed shedding frequency results in a decreasing Strouhal number. The bridge natural frequency, not the wind velocity, controls the shedding frequency. As wind velocity increases, the lock-in phenomenon disappears and the vibration reduces to a small amplitude (Figure 3.3.b). The shedding frequency may lock in another higher natural frequency (N2) at higher wind velocity. Therefore, many wind velocities can cause vortex shedding.

To describe the above mentioned experimental observation, much effort has been made to find an expression for forces resulting from vortex shedding. Since the interaction between the wind and the structure is very complex, no completely successful model has yet been developed for bridge sections. Most models deal with the interaction of wind with circular sections. A semi-empirical model for the lock-in is given as seen below

$$m\ddot{y} + c\dot{y} + ky = \frac{1}{2}\rho U^2 (2D)\left[Y_1(K)\left(1 - \varepsilon \frac{y^2}{D^2}\right)\frac{\dot{y}}{D} + Y_2(K)\frac{y}{D} + \frac{1}{2} C_L(K)\sin(\omega t + \phi)\right] \quad \textbf{(3.3)}$$

where k=Bω/Ū= reduced frequency; Y1, Y2, ε, and CL = parameters to be determined from experimental observations. The first two terms of the right side account for the motion-dependent force. More particularly, the first term accounts for aerodynamic damping and y term for aerodynamic stiffness. The ε accounts for the nonlinear aerodynamic damping to ensure the self-limiting nature of vortex shedding. The last term represents the instantaneous force from vortex shedding alone which is sinusoidal with the natural frequency of bridge. Solving the above given derived equation gives the vibration [2].

Vortex shedding occurs in both laminar and turbulent flow. According to some experimental observations, turbulence helps to break up vortices and therefore helps to suppress the vortex shedding response. A more complete analytical model must consider the interaction between modes, the spanwise correlation of aerodynamic forces and the effect of turbulence.

For a given section shape with a known Strouhal number and natural frequencies, the lock-in wind velocities can be calculated with Eq. (3.3). The calculated lock-in wind velocities are usually lower than the maximum wind velocity at bridge sites. Therefore, vortex shedding is an inevitable aerodynamic phenomenon. However, vibration excited by vortex shedding is self-limited because of its nonlinear nature. A relatively small damping is often sufficient to eliminate, or at least reduce, the vibrations to acceptable limits.

Although there are no acceptance criteria for vortex shedding in the design specifications and codes in the United States, there is a common agreement that limiting acceleration is more appropriate than limiting deformation. It is usually suggested that the acceleration of vortex shedding is limited to 5% of gravity acceleration when wind speed is less than 50 km/h and 10% of gravity acceleration when wind speed is higher. The acceleration limitation is then transformed into the displacement limitation for a particular bridge [2].

3.5 Galloping

“Galloping” is the term used to describe large amplitude vibrations occurring in a direction normal to the mean wind at frequencies much lower than those of vortex shedding from the structure[2].

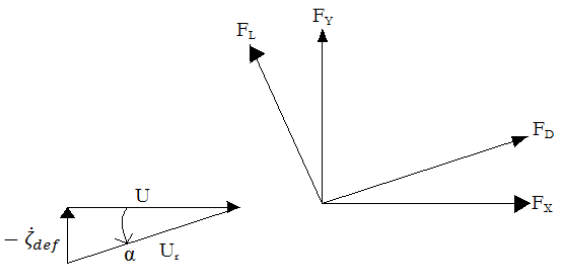

Figure 3.4 : Directions of forces in galloping and angle of attack.

Galloping is a common instability mode for transmission lines that have non-circular cross-sections due to particular reasons. It can happen to some forms of bridges, usually those with light weight, but it is not a typical instability mode for long-span cable-supported bridges.

Galloping usually occurs at very low reduced frequencies, Bv=Ū, where B is the typical chord or deck width dimension, v is the frequency of vibration and Ū is the mean of the free stream velocity. Because the reduced frequency is low, the aerodynamic pressure or force on the bridge deck can be assumed to vary with the incoming velocity in the same manner as for steady flow (the quasi-steady assumption). Therefore, mean or average static aerodynamic data (lift and drag coefficients) can be used to assess the susceptibility of a particular bridge deck to the galloping phenomena.

When a steady wind flow passes an oscillating structure, the effective angle of attack changes with the motion of the structure, even if the incoming flow has a fixed angle of attack. The changing effective angle of attack results in the change of aerodynamic forces and leads to self-excited forces. Consider a 2-D steady flow passing a structure section, as shown in Figure 3.5.

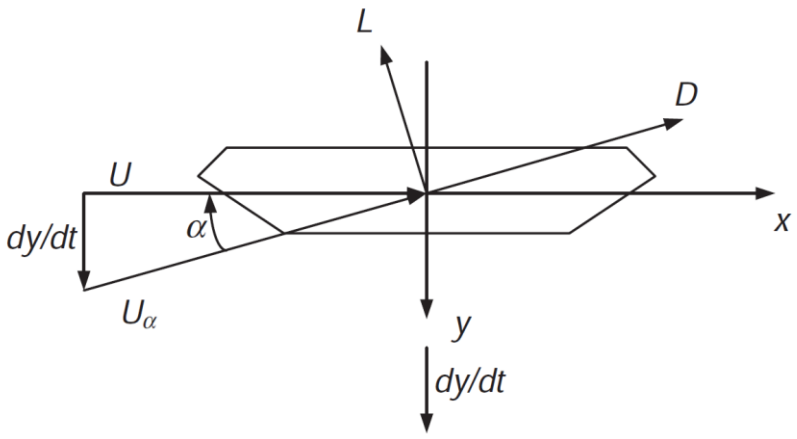

Figure 3.5 : Schematic diagram for 2-D steady flow-induced galloping.

Although the incoming flow velocity U is horizontal, the actual wind velocity acting on the structure is U, with an effective angle of attack, because of the motion of the structure in the y-direction. Based on the quasi-steady assumption, the drag and lift forces can be expressed as:

$$D(\alpha) = 1/2\rho U_\alpha^2 B C_D(\alpha) \qquad \textbf{(3.4)}$$

$$L(\alpha) = 1/2\rho U_\alpha^2 B C_L(\alpha) \qquad \textbf{(3.5)}$$

where:

D(α) and L(α) are the drag and lift forces on the structure section, respectively; U_α is the wind velocity with effective angle of attack α; B=2b is the bridge deck width; $C_D(\alpha)$ and $C_L(\alpha)$ are the drag and lift coefficients of the structure section, respectively. ρ is the air density.

4. AIRFOIL FORCES AND DESIGN

4.1 Introduction to Steady Aerodynamics

Aircrafts are able to fly because the lift generated by the airflow over the wings, and horizontal tail surfaces supports their weight. For a flexible aircraft, these lift forces give rise to deflections in the aerodynamic shape, which in turn change the characteristics of the airflow, hence leading to aeroelastic phenomena and affecting the dynamic loads. An understanding of how the aerodynamic flow around a two-dimensional aerofoil (i.e. the section of a typical wing profile), or a three-dimensional aerodynamic surface, generates the forces and moments that occur during flight is very important in order to be able to develop mathematical models that describe the aeroelastic behaviour [8].

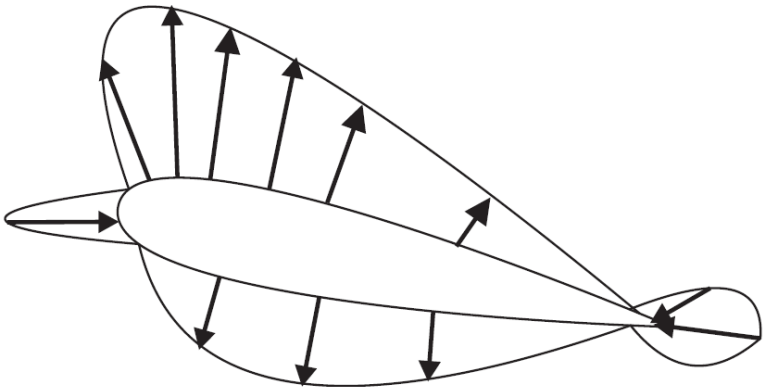

Figure 4.1 : Typical pressure distribution for a symmetric aerofoil at a small angle of incidence.

4.2 Aerofoil

An airfoil is the shape of a wing, blade (of a propeller, rotor, or turbine), or sail. An airfoil-shaped body moves through a fluid produces an aerodynamic force. The component of this force perpendicular to the direction of motion is called lift. The component parallel to the direction of motion is called drag. Subsonic flight airfoils have a characteristic shape with a rounded leading edge, followed by a sharp trailing

edge, often with a symmetric curvature of upper and lower surfaces. Foils of similar function designed with water as the working fluid are called hydrofoils.

Airfoil terminology;

i) The suction surface (a.k.a. upper surface) is generally associated with higher velocity and lower static pressure.

ii) The pressure surface (a.k.a. lower surface) has a comparatively higher static pressure than the suction surface. The pressure gradient between these two surfaces contributes to the lift force generated for a given airfoil.

iii) The leading edge is the point at the front of the airfoil that has maximum curvature (minimum radius).

iv) The trailing edge is defined similarly as the point of maximum curvature at the rear of the airfoil.

v) The chord line is the straight line connecting leading and trailing edges. The chord length, or simply chord, c, is the length of the chord line that is the reference dimension of the airfoil section.

vi) The mean camber line or mean line is the locus of points midway between the upper and lower surfaces. Its shape depends on the thickness distribution along the chord.

vii) The aerodynamic center, which is the chord-wise length about which the pitching moment is independent of the lift coefficient and the angle of attack.

viii) The center of pressure, which is the chord-wise location about which the pitching moment is zero.

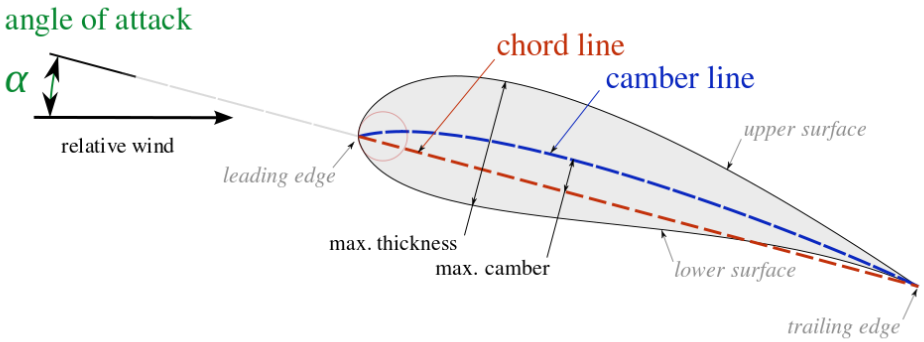

Figure 4.2 : Airfoil nomenclature

4.3 Forces on an Aerofoil

For an aerofoil moving at velocity V in a fluid at rest, the pressure distribution acting over the surface of the aerofoil gives rise to a total force. The position on the chord at which the resultant force acts is called the centre of pressure, as shown in Figure 4.5. If the angle of incidence α (angle between the mean airflow and the chord line of the aerofoil, measured in radians) alters, then the pressure distribution over the aerofoil changes, which leads to a repositioning of the centre of pressure. The changing centre of pressure position with respect to different angles of incidence leads to difficulties in any simple aeroelastic analysis, since the forces and moments need to be recalculated continually. For convenience, the net force is usually replaced by two resultant orthogonal forces, acting at a chosen reference point on the aerofoil, and a moment as seen in Figure 5.4.

The lift (L) is the force normal to the relative velocity of the aerofoil and fluid, the drag (D) is the force in the direction of relative velocity of the aerofoil and fluid, and the pitching moment (M) is the moment due to offset between the centre of pressure and the reference point (positive when pushing the nose upwards as shown in Figure 4.3). It is usual to use non-dimensional coefficients which relate the above quantities to the dynamic pressure and chord for a unit span of aerofoil (since it is two-dimensional), so that the lift, drag and moment coefficients are defined as

$$C_{\mathrm{L}} = \frac{\text{Lift } L}{\frac{1}{2}\rho V^2 c} \qquad C_{\mathrm{D}} = \frac{\text{Drag } D}{\frac{1}{2}\rho V^2 c} \qquad C_{\mathrm{M}} = \frac{\text{Pitching moment } M}{\frac{1}{2}\rho V^2 c^2} \tag{3.6}$$

respectively, where c is the aerodynamic aerofoil chord and the lift, drag and pitching moments are defined per unit span of the aerofoil. It is often more useful to use the coefficients rather than the total lift, drag and pitching moment per unit span as they are normalized by dynamic pressure and the aerofoil chord. Note that the forces and pitching moment can be defined with reference to any point on the chord [5].

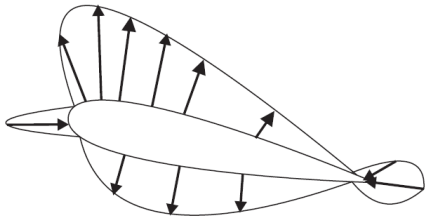

Figure 4.3 : Typical pressure distribution for a symmetric aerofoil at a small angle of incidence.

4.3.1 Lift force

A fluid flowing past the surface of a body exerts a force on it. Lift is the component of this force that is perpendicular to the oncoming flow direction.[1] It contrasts with the drag force, which is the component of the surface force parallel to the flow direction. If the fluid is air, the force is called an aerodynamic force. In water, it is called a hydrodynamic force.

4.3.2 Drag force

In fluid dynamics, drag (sometimes called air resistance, a type of friction, or fluid resistance, another type of friction or fluid friction) refers to forces acting opposite to the relative motion of any object moving with respect to a surrounding fluid.[1] This can exist between two fluid layers (or surfaces) or a fluid and a solid surface. Unlike other resistive forces, such as dry friction, which are nearly independent of velocity, drag forces depend on velocity.[2][3] Drag force is proportional to the velocity for a laminar flow and the squared velocity for a turbulent flow. Even though the ultimate cause of a drag is viscous friction, the turbulent drag is independent of viscosity.[11]

4.4 Effect of Air Speed on Aerodynamic Characteristics

The airflow and the resulting pressure distribution around a two-dimensional aerofoil changes depending upon the air speed and altitude. These characteristics can be defined in terms of several dimensionless quantities.

4.4.1 Mach number

One particularly important influence upon the characteristics of all fluid flows is the compressibility of the air, which alters depending upon the ratio between the local flow velocity V at some point in the flow and the speed of sound a. This ratio is known as the Mach number (M) and is defined as

$$M = \frac{V}{a} \qquad \textbf{(3.7)}$$

The value of M has a significant effect on the flow characteristics around aerofoils and aerodynamic surfaces, and specific flow regimes can be defined approximately as shown in Table 4.1.

Table 4.1: Mach number table

Type of Surface	**z_0(mm)**	**A**	
M < 0.75	Subsonic	No schoks present in the flow	Gliders / propeller aircraft / some jet transports
0.75 < M <1.2	Transonic	Shocks are attached to the airfoil	Civil transports
M = 1	Sonic	Flow at the speed of sound	Fighter aircraft
1.2 < M < 5	Supersonic	Shock present but not attached to the airfoil	Fighter aircraft
M > 5	Hypersonic	Viscous interaction, entropy layer, high temperature effects become	Missiles

4.4.2 Reynolds number

The Reynolds Number (Re) is a further non-dimensional quantity that influences the flow around aerofoils and is defined as

$$Re = \frac{\rho V c}{\mu} \qquad \textbf{(3.8)}$$

where c and μ are the aerofoil chord and air viscosity respectively while ρ is air density. The Reynolds number defines whether a viscous flow, particularly in the boundary layer (the region close to the aerofoil surface where the flow velocity is slowed down due to surface friction) is laminar (i.e. flow velocity varies smoothly close to the surface of the aerofoil) or turbulent (i.e. flow velocity varies randomly

and irregularly close to the surface). The Reynolds number represents the ratio of inertia to viscous forces in the flow.

4.4.3 Dynamic pressure

The dynamic pressure q is defined as ½ ρV2, where the air density ρ and velocity V need to be defined consistently. It is common practice to define velocity in terms of the equivalent air speed V_{EAS}, which is the speed at sea level that gives the same dynamic pressure as at some altitude, i.e.

$$\frac{1}{2}\rho V^2 = \frac{1}{2}\rho V_{EAS}^2 \rightarrow V_{EAS} = \sqrt{\frac{\rho 1}{\rho_0}} V = \sqrt{\sigma} * V \qquad \textbf{(3.9)}$$

where σ is the ratio of the air density at some altitude to the sea level air density ρ0. Strictly, V should be referred to as VTAS, the true air speed. These air speeds will be referred to later in the book when aeroelasticity and loads are considered. Note that speed is sometimes referred to in knots (nautical miles per hour); the conversion factors are 1 knot to 0.5144 m/s or 1.1508 mph.

5. ANALYSIS AND RESULTS OF THE WING STRUCTURE

5.1 Introduction

In this section the necessary forces, structural elements of the wing and supports will be designed for the wing design. Each wing is 20m long and 3.8m wide.

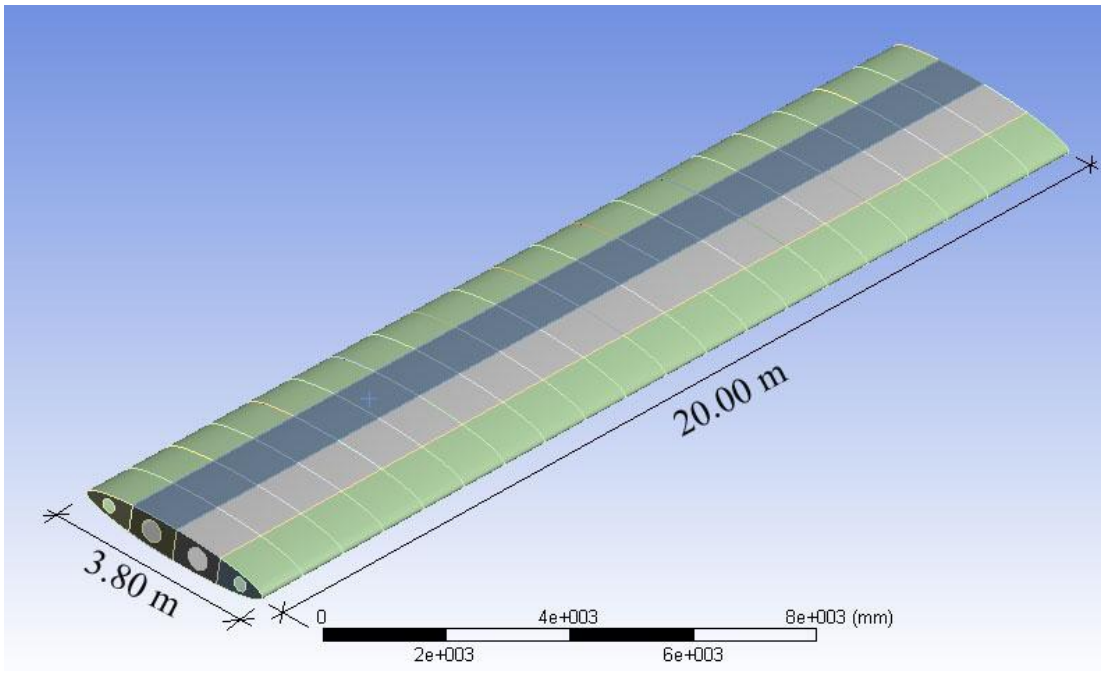

Figure 5.1 : The geometry of the wing.

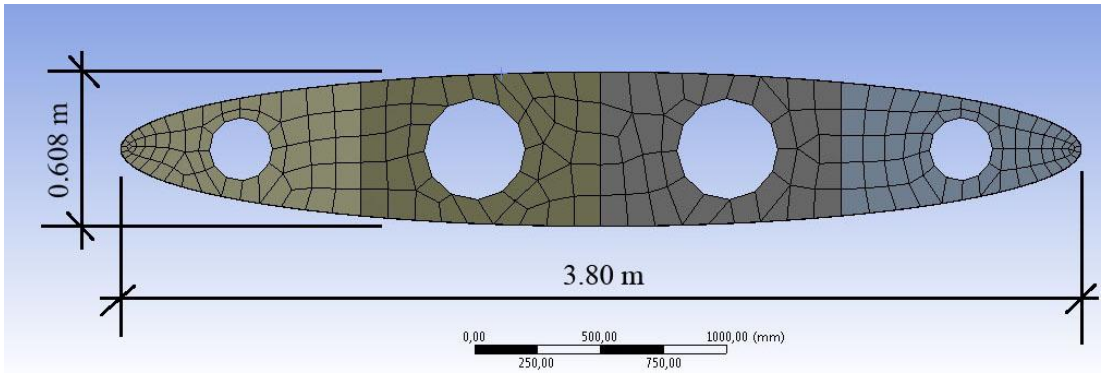

Figure 5.2 : The cross section of the wing.

5.2 The Parameters and Necessary Knowledge from Former Study

There were four wing configurations had been selected. Table 5.1 contains information on the variations with respect to the dimensions and the impact on the critical wind speed of the bridge.

Table 5.1: Wing configurations

	$\tilde{a}$	$\tilde{b}$	Max. Projection [m]	Leaf Width [m]	Raising from v_k [%]	Δv_c [m/s]
A.1	1,5	0,1	9,5	3,8	23,5	10,9
A.2	1,5	0,05	9,5	1,9	11,8	5,4
B.1	2	0,1	19,0	3,8	Fluttering-satable	Fluttering-satable
B.2	2	0,05	19,0	1,9	18,6	8,6

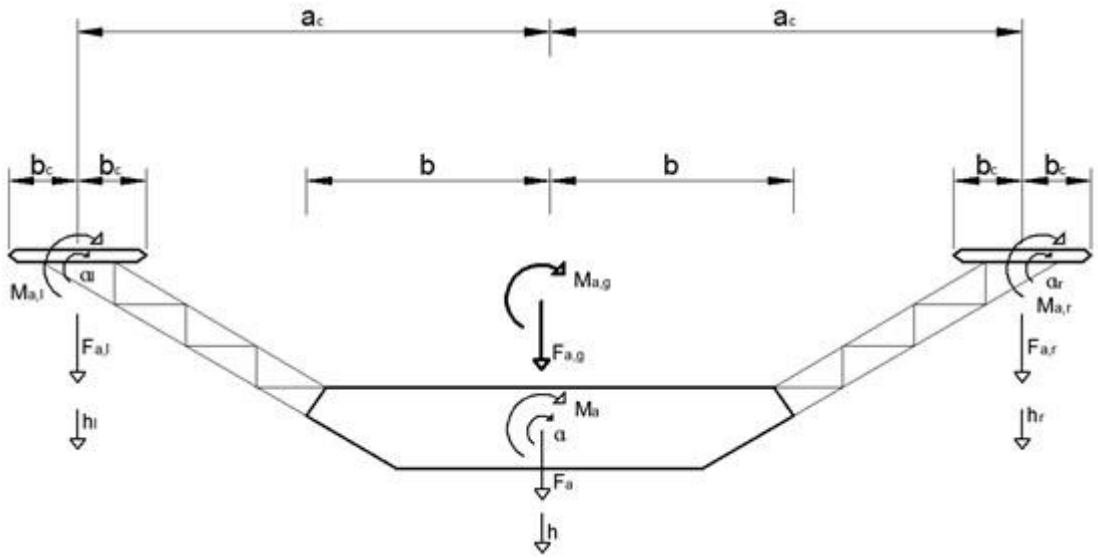

Figure 5.3: Air force sizes on the wing system

$$\tilde{b} = \frac{b_c}{b} \qquad \textbf{(5.1)}$$

$$\tilde{a} = \frac{a_c}{b}, \qquad \textbf{(5.2)}$$

5.3 Wind Actions on Elliptical Airfoil Section

Wind forces has been calculated by a commercial software called XFLR5 which is an analysis tool for airfoils, wings and planes operating at low Reynolds Numbers.

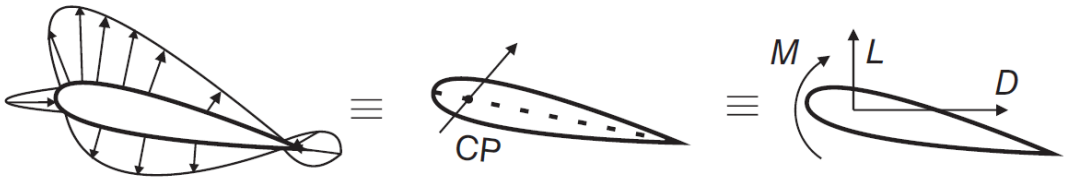

Figure 5.4: Resultant aerodynamic force acting at the centre of pressure CP.

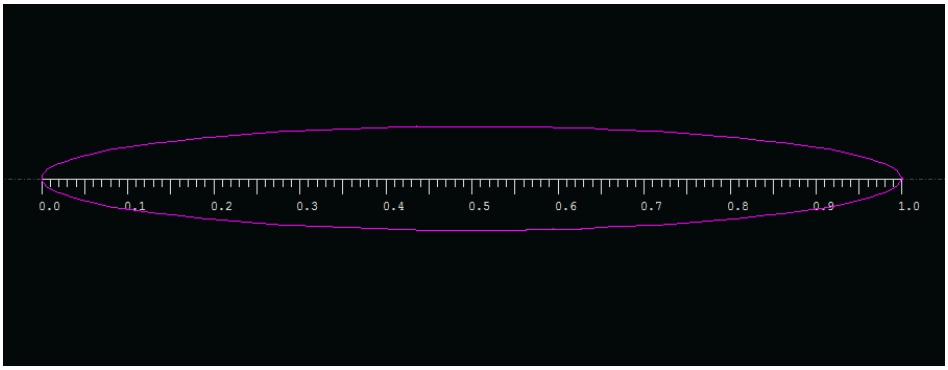

Figure 5.5: Elliptic airfoil unit width modelled for XFLR5

Table 5.2: Airfoil Properties

Airfoil Properties (m, m/sn)		
Airfoil Type	Elliptical	Unit
Velocity	59,3	m/s
Altitude	Sea Level	
Wing Span	20,00	m
Chord Length	3,80	m
Sweep	0°	
Wing Area	76	m^2
Wing Weight	1250	kg
Density	1,225	kg/m^3
Thickness	16% of width	
at %	50% of width	
Camber	0%	
at %	0%	

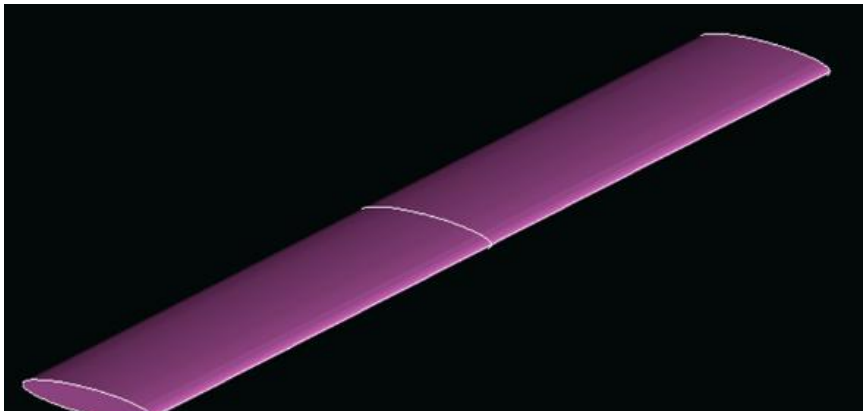

Figure 5.6: Illustration of the elliptical sectional wing on XFLR5

Table 5.3: Forces on an aerofoil for positive angle attack.

Alpha, α	C_L	C_D	C_M	L (kN) Lift	D (kN) Drag	M (kN*m) Pitching Moment
0	0,000502	0,010202	-0,0001	0,082	1,670	-0,064
1	0,066844	0,010476	-0,01339	10,942	1,715	-8,328
2	0,133187	0,01131	-0,02667	21,802	1,851	-16,588
3	0,19953	0,012705	-0,03993	32,662	2,080	-24,835
4	0,265872	0,014659	-0,05316	43,521	2,400	-33,067
5	0,332215	0,017173	-0,06636	54,381	2,811	-41,276
6	0,398557	0,020248	-0,07951	65,241	3,314	-49,457
7	0,4649	0,023882	-0,09261	76,101	3,909	-57,605
8	0,531249	0,028077	-0,10565	86,962	4,596	-65,718
9	0,597421	0,0329	-0,11855	97,793	5,385	-73,744
10	0,658204	0,03776	-0,1285	107,743	6,181	-79,933
11	0,703342	0,041341	-0,1295	115,132	6,767	-80,552
12	0,76192	0,047009	-0,13786	124,721	7,695	-85,752
13	0,826533	0,053935	-0,14962	135,297	8,829	-93,070
14	0,887369	0,061056	-0,16346	145,256	9,994	-101,678
15	0,9488	0,068955	-0,1773	155,312	11,287	-110,287

Table 5.3: Forces on an aerofoil for negative angle attack.

Alpha, α	C_L	C_D	C_M	L (kN)	D (kN)	M (kN*m)
-10	-0,65527	0,037652	0,127044	-107,263	6,163	79,025
-9	-0,59599	0,032954	0,118109	-97,560	5,394	73,468
-8	-0,53024	0,028165	0,105445	-86,797	4,610	65,590
-7	-0,4639	0,02396	0,092406	-75,936	3,922	57,479
-6	-0,39755	0,020315	0,079305	-65,077	3,325	49,330
-5	-0,33121	0,017229	0,066152	-54,217	2,820	41,149
-4	-0,26487	0,014704	0,052954	-43,357	2,407	32,939
-3	-0,19853	0,012738	0,039721	-32,497	2,085	24,708
-2	-0,13218	0,011333	0,026461	-21,637	1,855	16,460
-1	-0,06584	0,010487	0,013183	-10,778	1,717	8,200
0	0,000502	0,010202	-0,0001	0,082	1,670	-0,064

Only 2^o degree of angle of attack will be used in order to design the wing structure with its skin.

5.4 Building Up and Choosing the Structure of the Wing

The wing structure is made of three main structure members; skin, ribs and spars. With Ansys software Finite Element Method FEM will be used for determining the thickness of these members which are made of aluminum.

5.4.1 Wing spar

In a fixed-wing aircraft, the spar is often the main structural member of the wing, running spanwise at right angles (or thereabouts depending on wing sweep) to the fuselage. The spar carries vertical loads and the weight of the wings. Other structural and forming members such as ribs may be attached to the spar or spars, with stressed skin construction also sharing the loads where it is used. There may be more than one

spar in a wing or none at all. However, where a single spar carries the majority of the forces on it, it is known as the main spar.

5.4.2 Wing rib

Ribs are forming elements of the structure of a wing, especially in traditional construction. By analogy with the anatomical definition of "rib", the ribs attach to the main spar, and by being repeated at frequent intervals, form a skeletal shape for the wing. Usually ribs incorporate the airfoil shape of the wing, and the skin adopts this shape when stretched over the ribs.

Ribs are the structural crosspieces that combine with spars and stringers to make up the framework of the wing. They usually extend from the wing leading edge to the rear spar or to the trailing edge of the wing. The ribs give the wing its cambered shape and transmit the load from the skin and stringers to the spars. Similar ribs are also used in ailerons, elevators, rudders, and stabilizers.

5.4.3 Wing skin

Often, the skin on a wing is designed to carry part of the flight and ground loads in combination with the spars and ribs. This is known as a stressed-skin design.

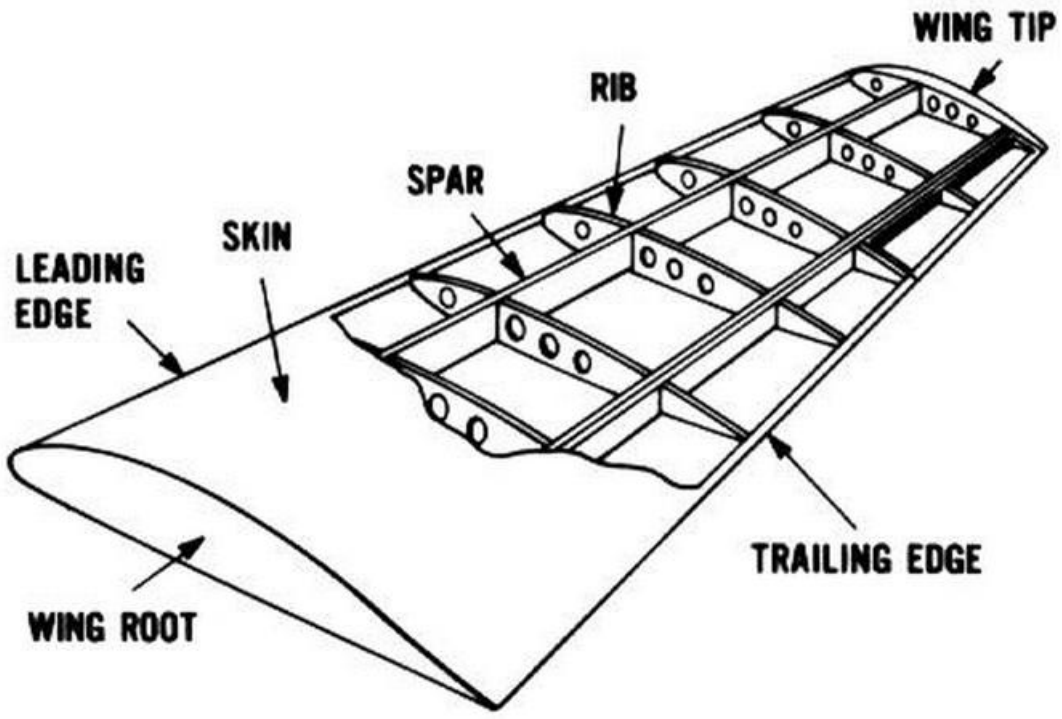

Figure 5.7: The memebers of a conventional wing structure

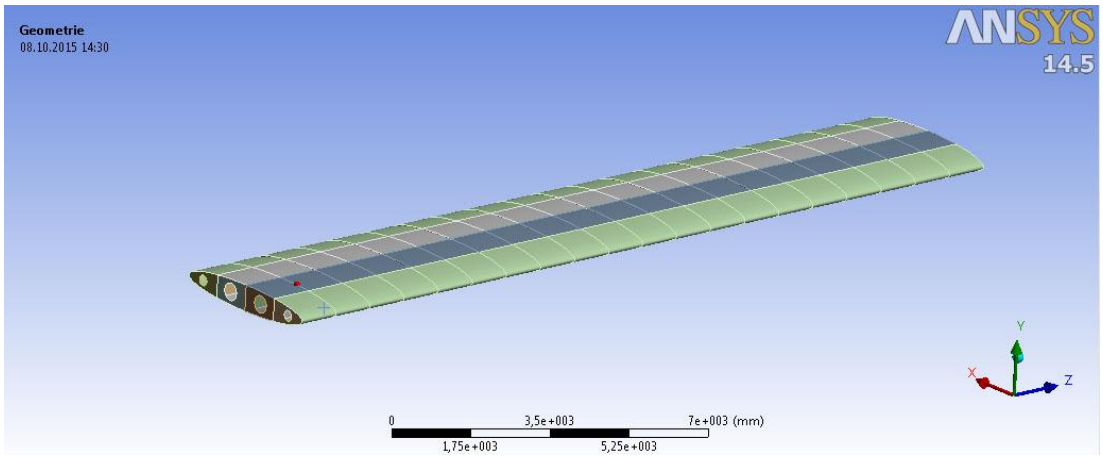

Figure 5.8: 3D view of the wing structure and the geometry

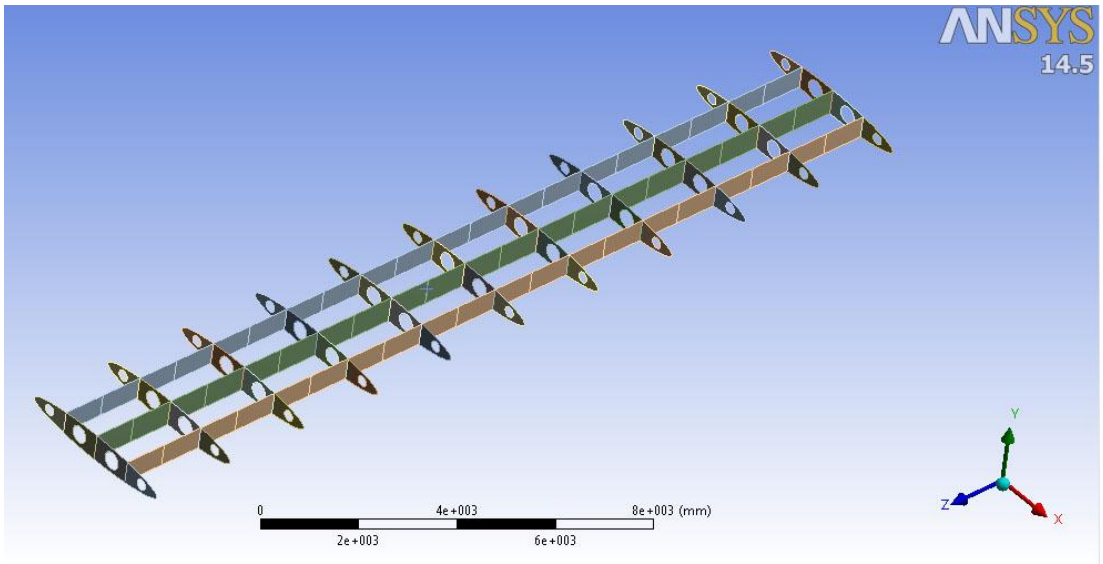

Figure 5.9: Framework of the wing structure

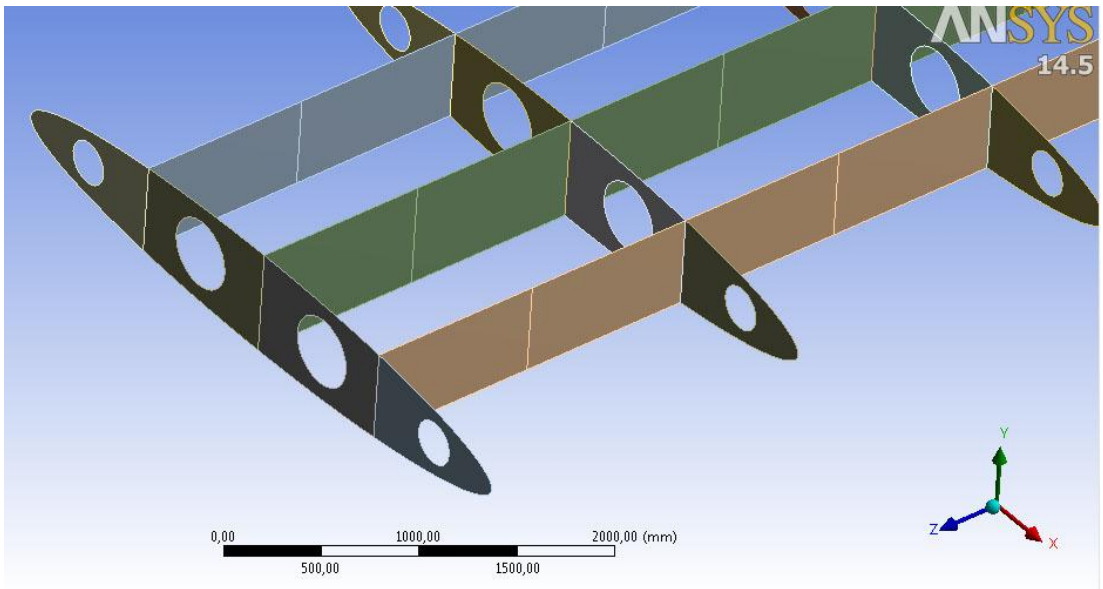

Figure 5.10: Framework of the wing structure, close view

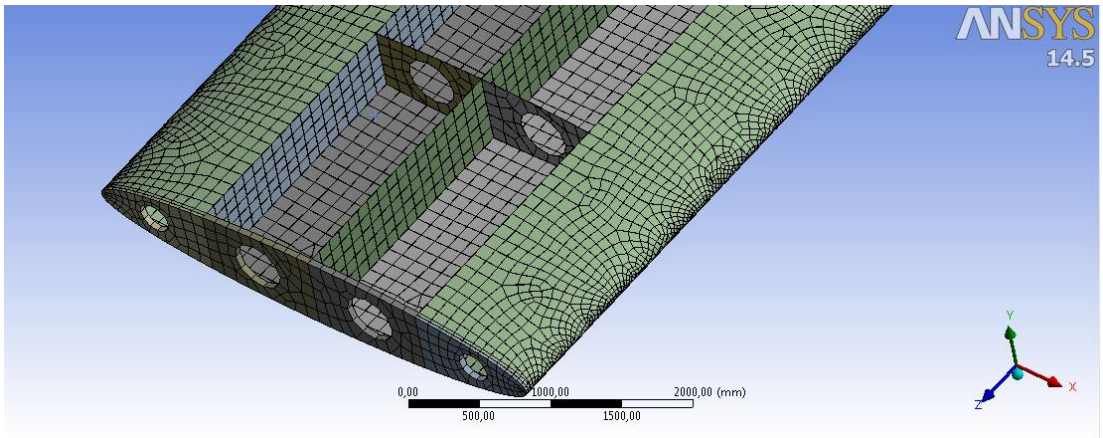

Figure 5.11: Meshed view of the model which has thicker edge ribs

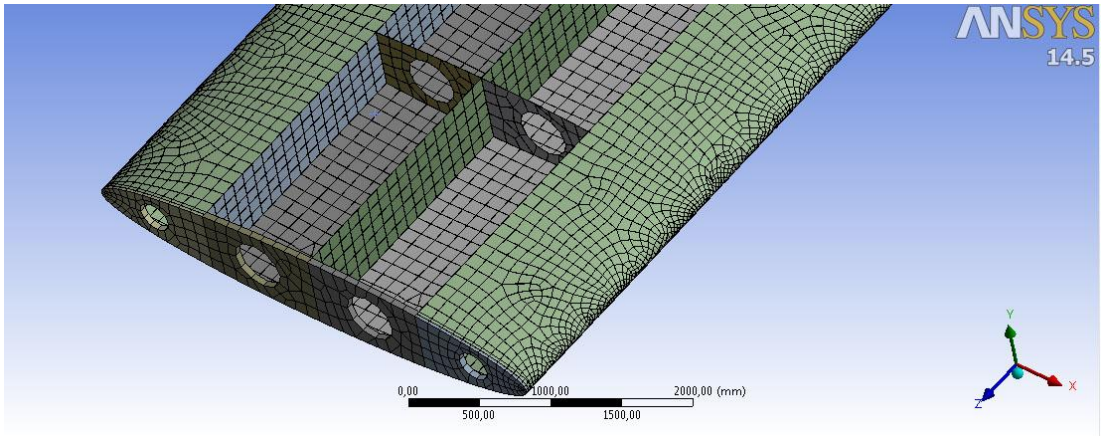

Figure 5.12: Meshed view of the model which has 2 mm edge ribs

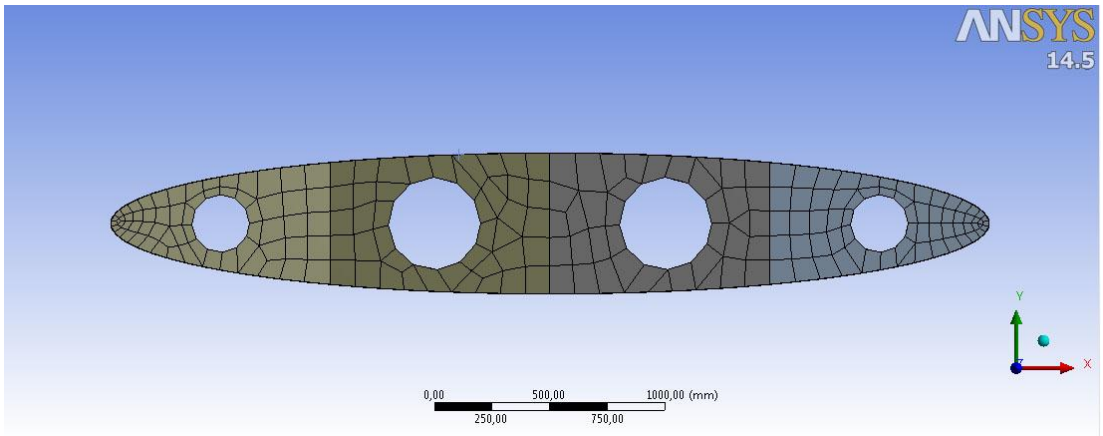

Figure 5.13: Meshing of ribss.

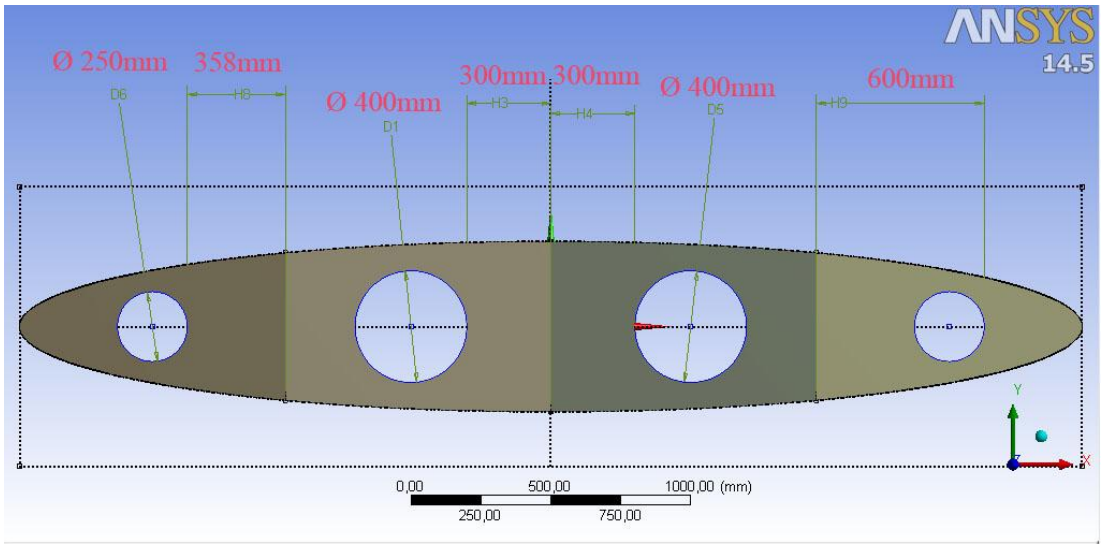

Figure 5.14: Dimensions of the rib and its gaps.

5.5 Load Design on Wing Structure

Load design was only considered for $\alpha=2^{o}$ angle of attack. The calculated point load values should be considered as distributed load in order to design the thickness of the material. In Finite Element Model, the angles of the lift and drag load and the positon were arranged accordingly.

Table 5.4 Forces which is occurred in 2^{o} degree of angle of attack.

Alpha, α	C_L	C_D	C_M	L (kN)	D (kN)	M (kN*m)
2	0,133187	0,01131	-0,02667	21,802	1,851	-16,588

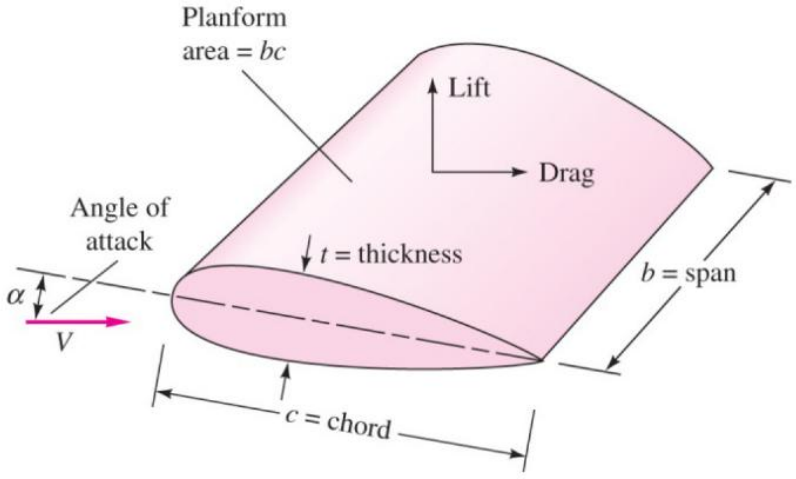

Figure 5.15: Definition sketch for an airfoil.

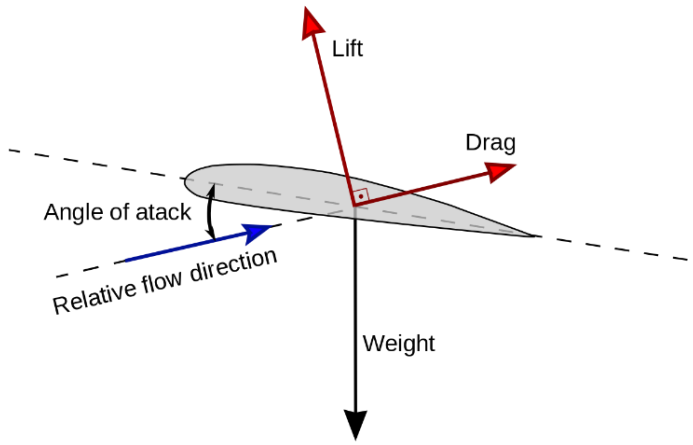

Figure 5.16: Lift and drag forces, lift force is always perpendicular to wind direction.

In any case of position of the section, lift force is always perpendicular to wing direction, and the drag force is every time in the same direction with the flow.

As for that modelling the wing on ANYSY software, since this rule is necessary to be applied, by keeping the position of the wing horizontal required the calculation of the vertical lift and the horizontal drag force according to ANSYS global directions.

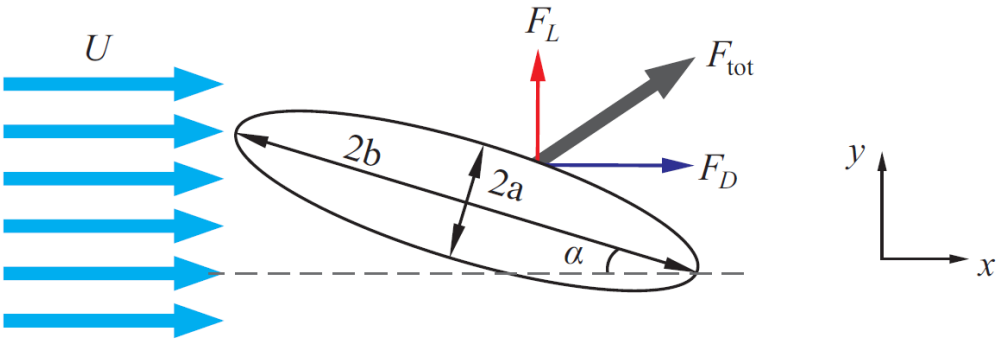

Figure 5.17: Lift and drag forces, lift force is always perpendicular to wind direction.

$$F_N = L * cos \propto + D * sin \propto \quad \textbf{(5.3)}$$

$$F_H = -L * sin \propto + D * cos \propto \quad \textbf{(5.4)}$$

$\propto = Angle\ of\ attack = 2^0$

L=Lift Force=21,802 kN

D=Drag Force=1,851 kN

M=Moment= -16,588 kNm

$$F_N = L * cos \propto + D * sin \propto$$

$$F_N = 21{,}802 * cos2 + 1{,}851 * sin2$$

$$F_N = 21{,}78 + 0{,}0165$$

$$F_N = 21{,}853\ kN$$

$$F_H = -L * sin \propto + D * cos \propto$$

$$F_H = -21{,}802 * sin2 + 1{,}851 * cos2$$

$$F_H = -0{,}76 + 1{,}85$$

$$F_H = 1{,}1\ kN$$

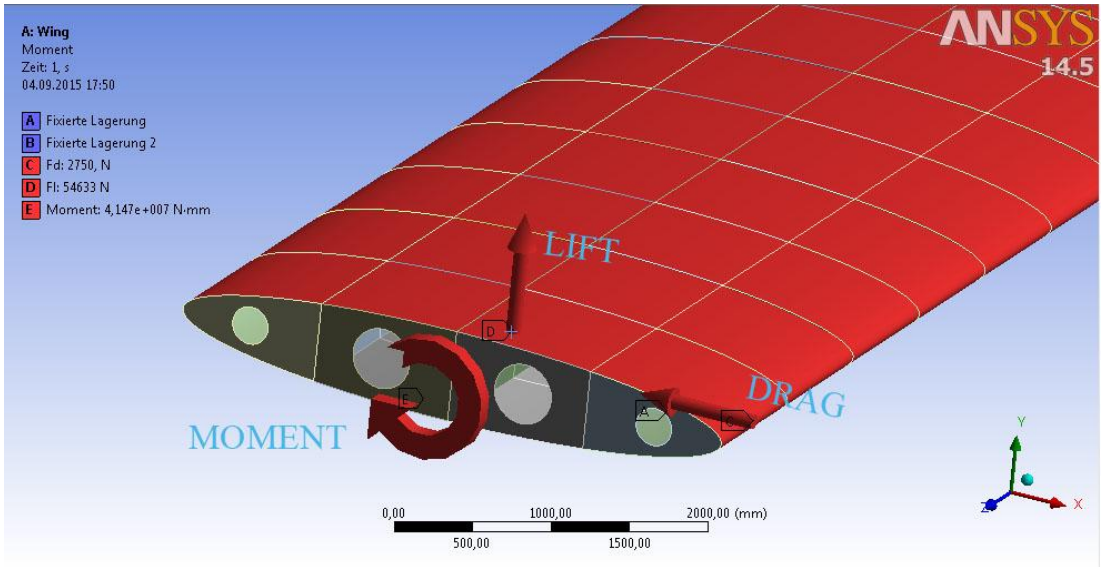

Figure 5.18: Forces acting on FEM of the wing.

$F_N = 21{,}853\ kN$

$F_H = 1{,}1\ kN$

$F_M = 16{,}588\ kNm$

$$N = L * cos \propto + D * sin \propto$$

FS: Factor of Safety

Factor of Safety: 2,5

$$FS * F_N = 2{,}5 * 21{,}853\ kN$$

$$FS * F_N = 54{,}633\ kN = 54633\ N$$

$$Lift\ Force = 54633\ N$$

Factor of Safety: 2,5

$$FS * F_H = 2{,}5 * 1{,}1\ kN$$

$$FS * F_H = 2{,}75\ kN = 2750\ N$$

$$Drag\ Force = 2750\ N$$

Factor of Safety: 2,5

$$FS * F_M = 2{,}5 * 16{,}588\ kNm$$

$$Moment = 41{,}47\ kNm$$

$$Moment = 4{,}147 * 10^7\ Nmm$$

Table 5.6: Distributed loads which are occurred in 2^o degree of angle of attack.

Alpha, α	C_L	C_D	C_M	Lift (N)	Drag (N)	M (N*mm)
2	0,133187	0,01131	-0,02667	54633	2750	$4{,}147*10^7$

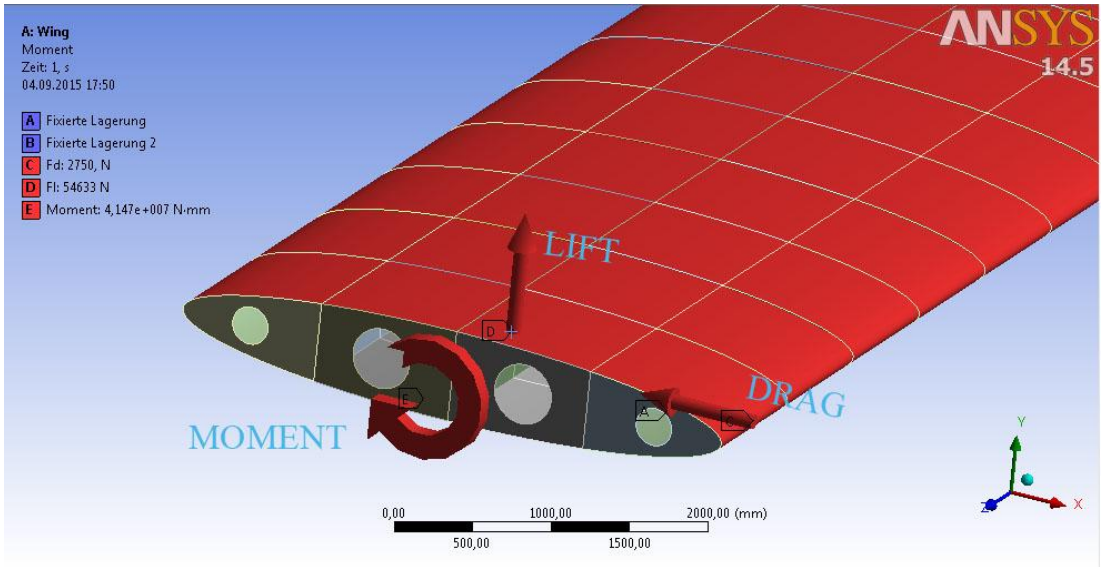

Figure 5.19: Getting forces loaded on skin of the wing.

5.6 Material Poperties

ANSYS software provides Finite Element Method in order to get the stress results, and by concerning these values the thickness can be calculated according to conventional strength calculation.

In order to have a light and cost efficient structure, it was decided to use aluminum material which is commonly used in aeroplane and car industries.

Material Grade: AeMg3Mn

Yield Strength: 85 MPa

Mechanical properties of grade ENAW-AlMg3Mn (ENAW-5454)

Table 5.7: Material properties.

AeMg3Mn	
Rm - Tensile strength (MPa) (H14)	270-325
Rm - Tensile strength (MPa) (F) (H112)	200
Rm - Tensile strength (MPa) (O) (H111)	200-275
Rp0.2 0.2% proof strength (MPa) (H14)	220
Rp0.2 0.2% proof strength (MPa) (F) (H112)	85
Rp0.2 0.2% proof strength (MPa) (O) (H111)	85
O	Annealed
H	Strain hardened
F	Fabricated (as cast)

ReH : Minimum yield strength

Rm : Tensile strength

A : Minimum elongation

J : Notch impact test

F : As fabricated. No mechanical property limits

O : Annealed To abtain the lowest strength highest ductility

H : Strain hardened. If necassary partially annealed to achieve designated mechanical properties

W : Solution heat treated. Unstable material condition

T : Thermally treated. To produce stable material condition

Nominal chemical compound % (acc. to the standard EN 573-1) are given below.

Table 5.8: Nominal chemical compound % (according to the standard EN 573-1).

Alloy numerical		EN AW-5454
Alloy chemical		EN AW-AlMg3Mn
Si		0,25
Fe		0,40
Cu		0,10
Mn		0,50-1,0
Mg		2,4-3,0
Cr		0,05-0,20
Zn		0,25
Ti		0,20
Others	Each	0,05
	Total	0,15
Al		Reste

EN 485-2: 2008 Aluminium and aluminium alloys. Sheet, strip and plate.

Table 5.9: Sheets (according to the standard EN 485-2).

Numerical EN designation	**Chemical designation**			
EN AW-	EN AW-	sheet	extrusions	forgings
5454	AlMg3Mn	✓	✓	✓

Table 5.10: The designation of the material conditions are specified in DIN EN 515.

Numerical	EN AW-5454
Chemical symbols	EN AW-AlMg3Mn
Density (g/cm3)	2,68
(GPa) Young's Modulus	70
20-200°C [10-6K] Coefficient of thermal expansion	23,7
[W/K·m] Thermal conductivity 20°C [MS/m]	120 - 130
Electrical conductivity	16 - 19

Table 5.11: Sheets (according to the standard EN 485-2).

State	**Specified thickness**		**Rm (MPa)**		**Rp0,2 (MPa)**		**A %**		**Bending radius**		**Hardness HBS**
	More than	Until	min	max	min	max	A 50	A	180°	90°	
F	2,5	80	215	-	-	-	-	-	-	-	-
O/H111	0,2	0,5	215	275	85	-	12		0,5 t	0,5 t	58
	0,5	1,5	215	275	85		13		0,5 t	0,5 t	58
	1,5	3	215	275	85		15		1,0 t	1,0 t	58
	3	6	215	275	85		17			1,5 t	58
	6	12,5	215	275	85		18			2,5 t	58
	12,5	80	215	275	85			16			58

6. STRUCTURAL AND STRESS ANALYSIS

6.1 Structural and Stress Analysis of the Wing

The wing has been supported both simply supported and fixed supported for two different approchment and assembly.Initial and end ribs were supported in two different models.

First support conditions were considered as sliding in Z direction, fixed in X direction and Y direction. Also rotation is fixed around Z direction.

Second support conditions were arranged especially to keep the movement in Z direction. Supports have been fixed in three directions and the rotation around Z direction is fixed, too.

Material grade has been explained in detail in previous section and has been given briefly below.

Material Grade: AeMg3Mn

σ0.2 =85 MPa, Minimum yield strength

Rp0.2 0.2% proof strength (MPa) (F) (H112): 85 MPa

The thickness of the members has been decided as the following after a couple of analysis, and final strength results has been shown.

Skin: 2 mm

Ribs: 2 mm

Spars: 3mm

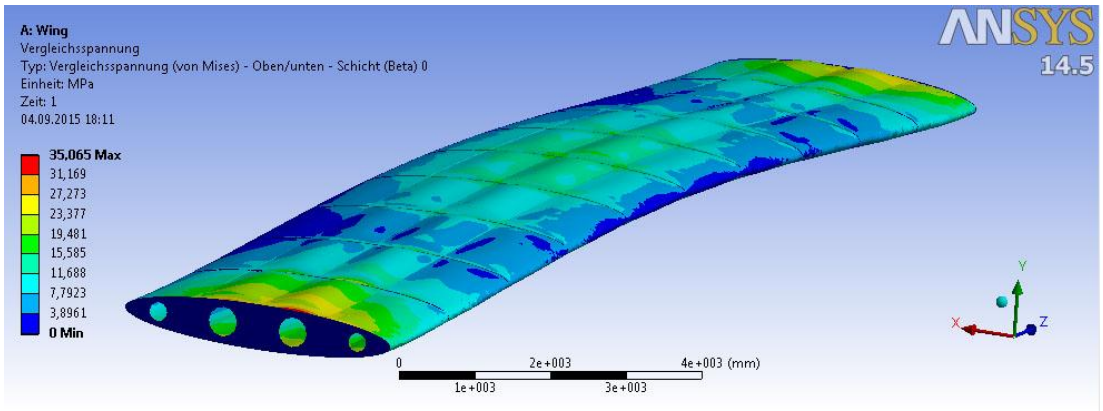

Figure 6.1: Equivalent Stress (view from second edge), Max: 35,065 MPa for simply supported model.

$$\sigma = 35{,}065 \text{ MPa} < \sigma_{yield} = 85 \text{ MPa}$$

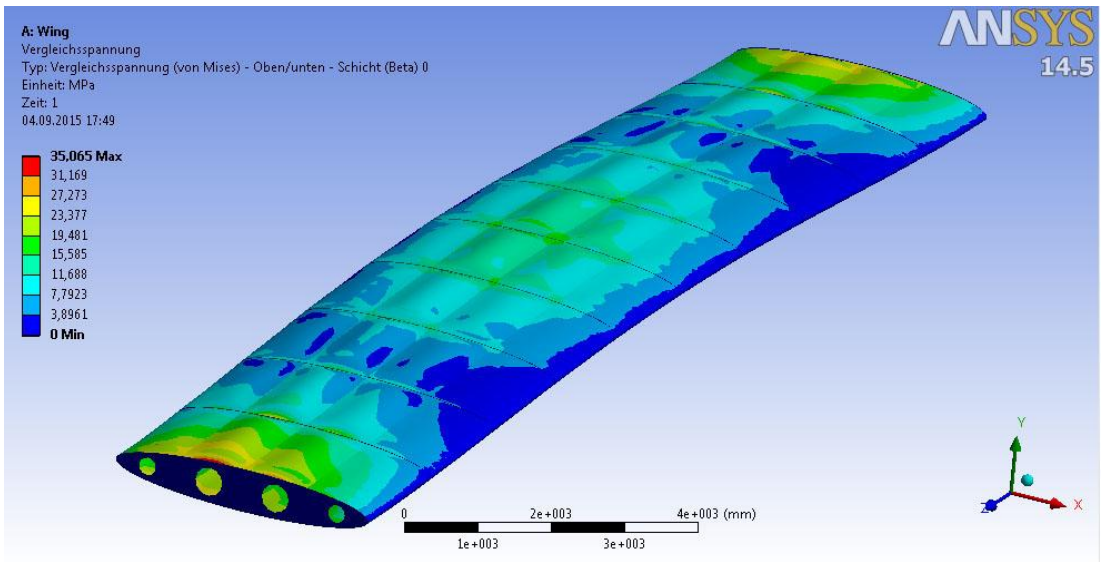

Figure 6.2 : Equivalent Stress (view from first edge), Max: 35,065 MPa for simply supported model.

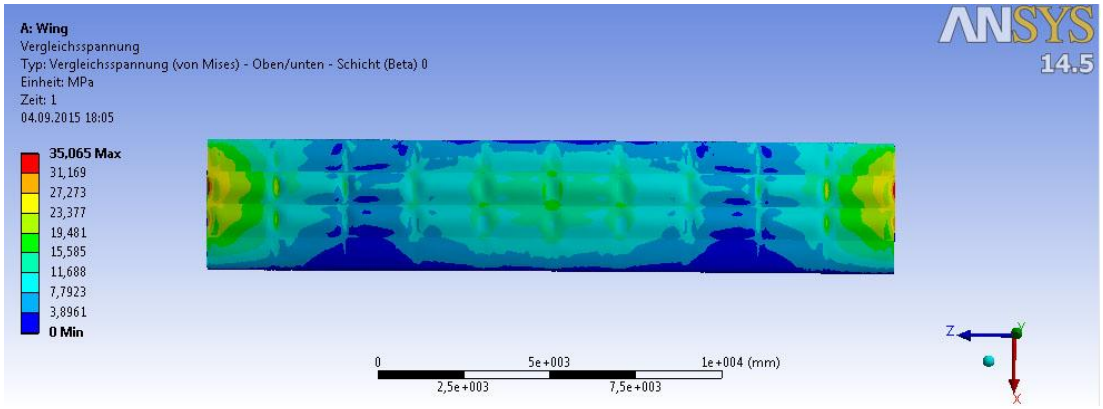

Figure 6.3 : Equivalent Stress (view from above), Max: 35,065 MPa for simply supported model. $\sigma = 35{,}065$ MPa$< \sigma_{yield} = 85$ MPa

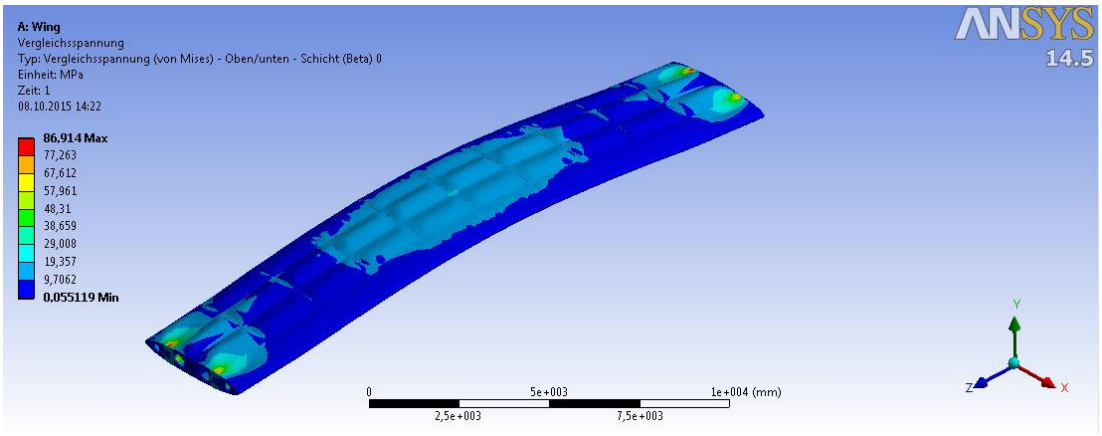

Figure 6.4 : Equivalent Stress, Max: 86,92 MPa for fixed supported model. $\sigma = 86{,}914$ MPa > $\sigma_{yield} = 85$ MPa

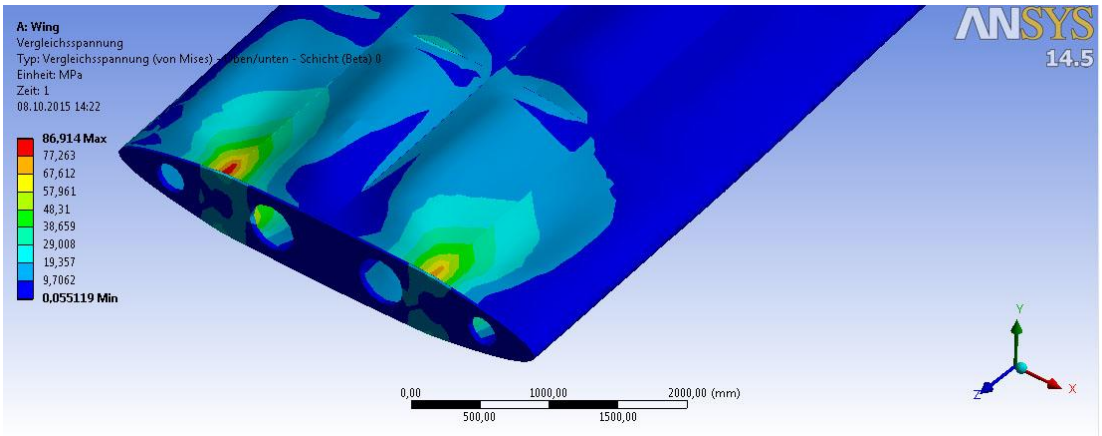

Figure 6.5 : Equivalent Stress, Max: 86,92 MPa for fixed supported model. $\sigma = 86{,}914$ MPa > $\sigma_{yield} = 85$ MPa

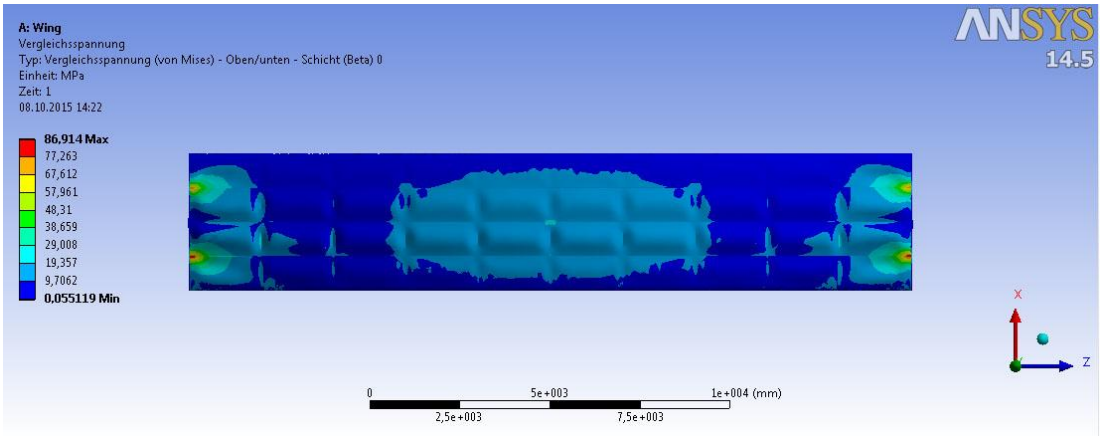

Figure 6.6 : Equivalent Stress, view from above Max: 86,92 MPa for fixed supported model. $\sigma = 86{,}914$ MPa > $\sigma_{yield} = 85$ MPa

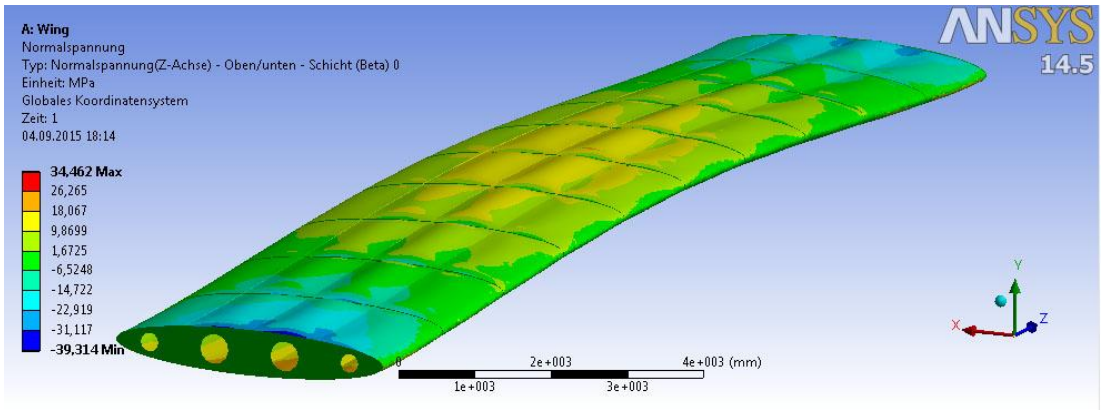

Figure 6.7 : Normal Stress, Max: 34,462 MPa for simply supported model.
$\sigma = 34{,}47$ MPa< $\sigma_{yield} = 85$ MPa

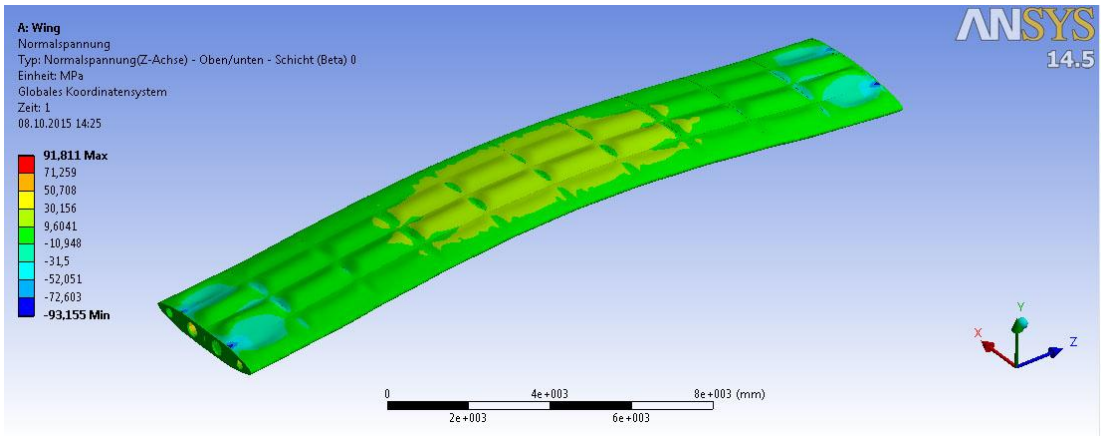

Figure 6.8 : Normal Stress, Max: 91,811 MPa for fixed supported model.
$\sigma = 91{,}82$ MPa > $\sigma_{yield} = 85$ MPa

Even though the normal stress is more than yield stress for fixed supported model, determined thicknesses can be even accepted, because the highest value has been observed nearby the edge ribs. Beside this, the forces was multiplied by 2.5 factor of safety in order to cover dynamic effects for furter calculations.

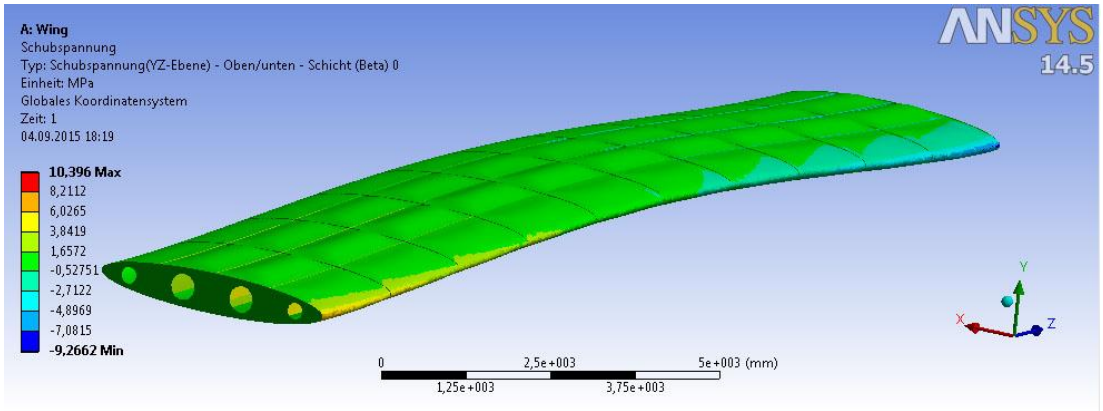

Figure 6.9 : Shear Stress, Max: 10,396 MPa for simply supported model.

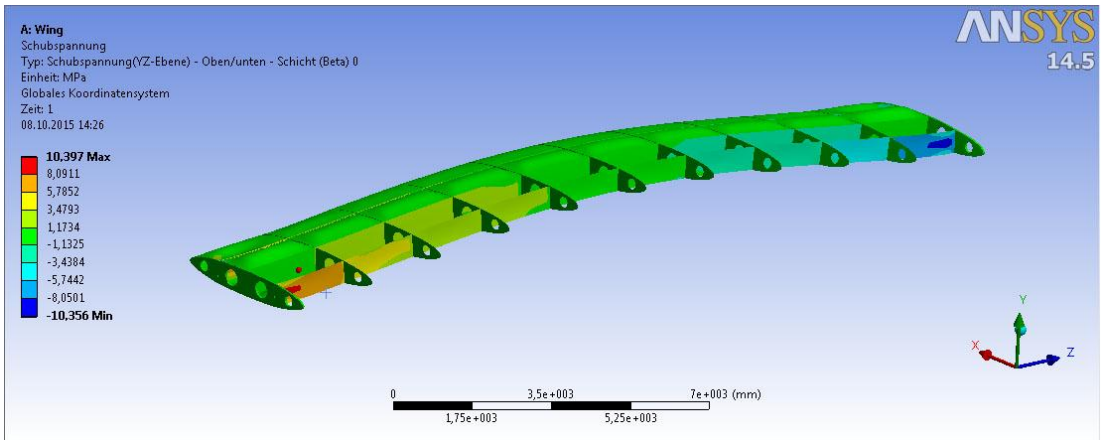

Figure 6.10: Shear Stress, Max: 10,397 MPa for fixed supported model.

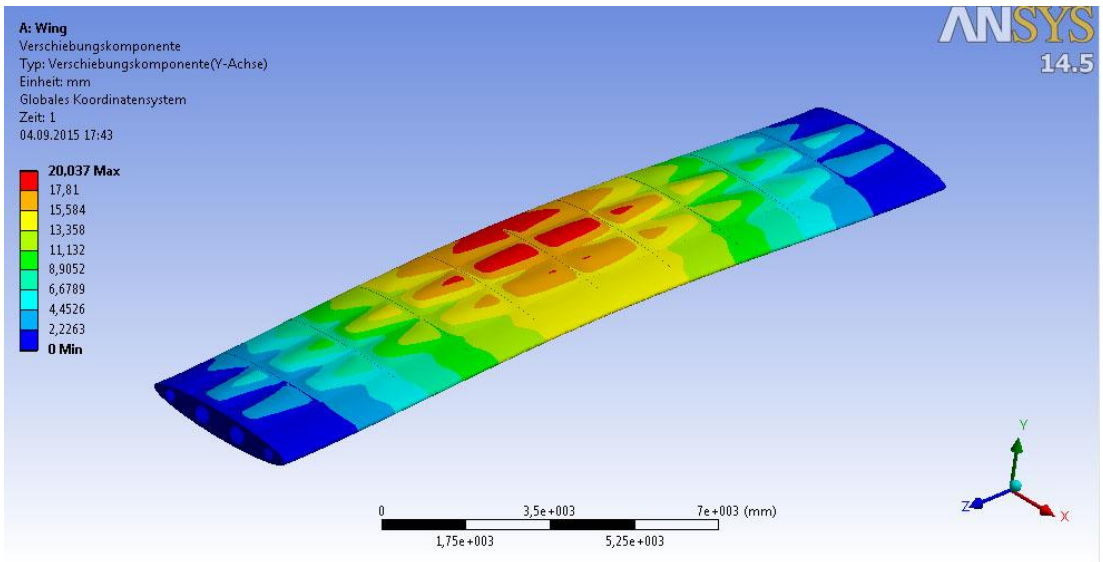

Figure 6.11: Deflection in gravity, Max: 20,04mm for simply supported model.

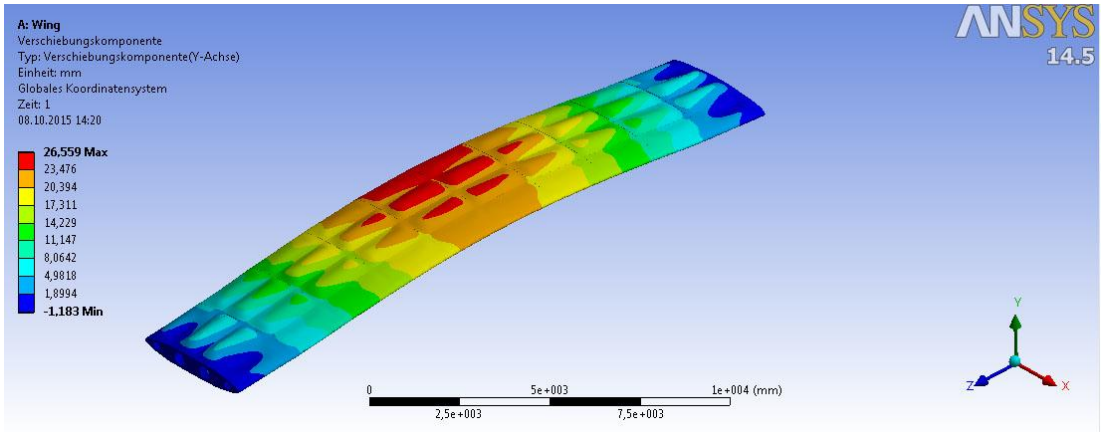

Figure 6.12: Deflection under gravity loads of the wing, Max: 26,56mm for fixed supported model.

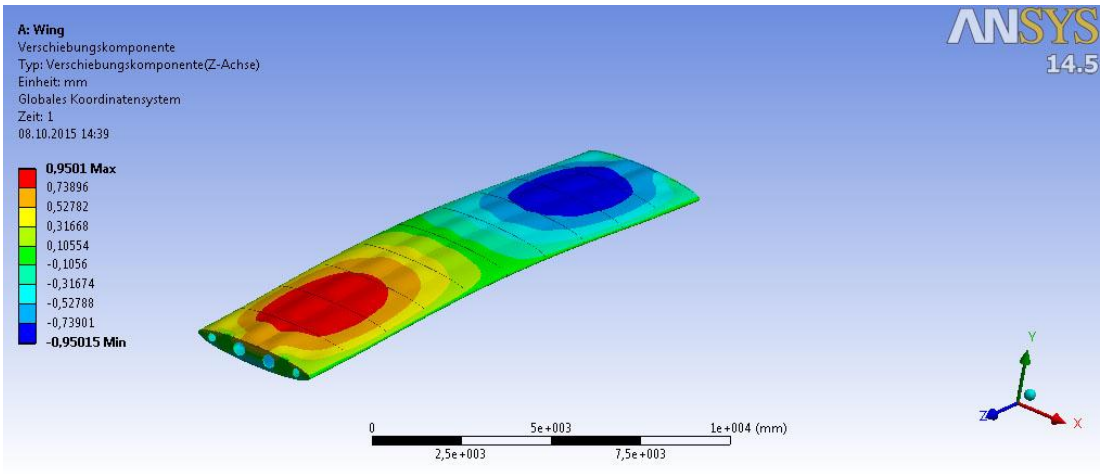

Figure 6.13: Deflection in direction Z, Max: 0,950mm for fixed supported model under the total wind forces.

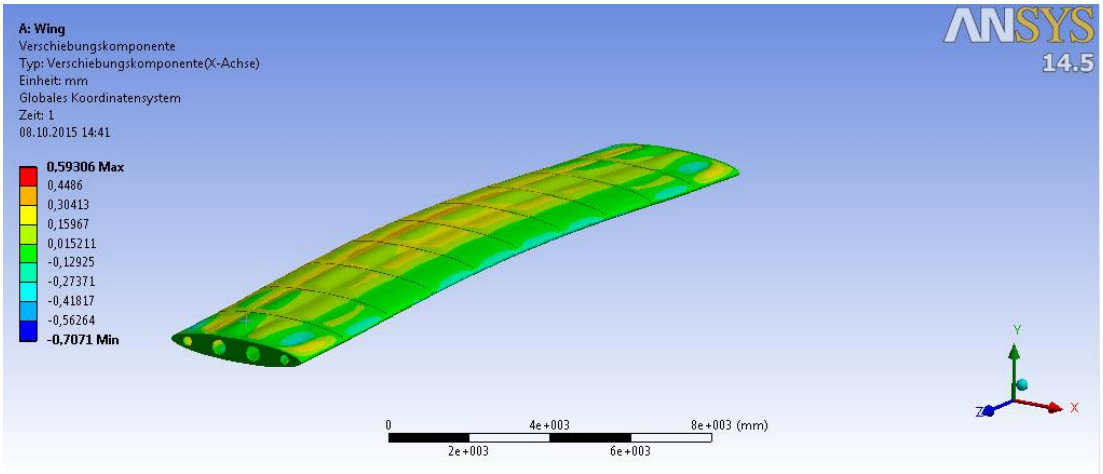

Figure 6.14: Deflection in direction X, Max: 0,593mm for fixed supported model under the total wind forces.

6.2 Structural and Stress Analysis of the Support

6.2.1 Introduction

In order to support the wing to bridge deck, a truss system has been choosen and designed, SAP2000 according to Eurocode. The purpose of this section is to explain all structural elements' design principals and all structural acceptances used.
As material, S235 has been assigned to profiles.

6.2.2 Units

SI international unit system (kN,m) is used for design and analysis.
Lenght (m)

Loads (kN)

Weight (kN)

Mass ($kN.sn^2/m$)

Moment (kN.m.)

Stress (kN/m^2)

6.2.3 Computer softwares

For this support's structural design SAP 2000 Ver 16.0.0 Computer Supported Design and Analysis Software is used. This software makes the design and calculations according to Finite Element Theory.

6.2.4 Materials & design parameters

The material coefficients to be adopted in calculations for the steels covered by this Eurocode shall be taken as follows:

Structural Steel S235JR according to EN 10025 (2004) for European pipe sections.

- Modulus of Elasticity : (Es) = 205000MPa
- Characteristic yield strenght: (σ_{yc})=235MPa
- Unit mass ρ = 7 850 kg/m^3
- Coefficient of linear thermal expansion α = 12 × 10–6 per °C
- Shear modulus G = E/2(1 + É)
- Poisson's ratio υ = 0,3
- Coefficient of linear thermal expansion α = 12 × 10–6 per °C

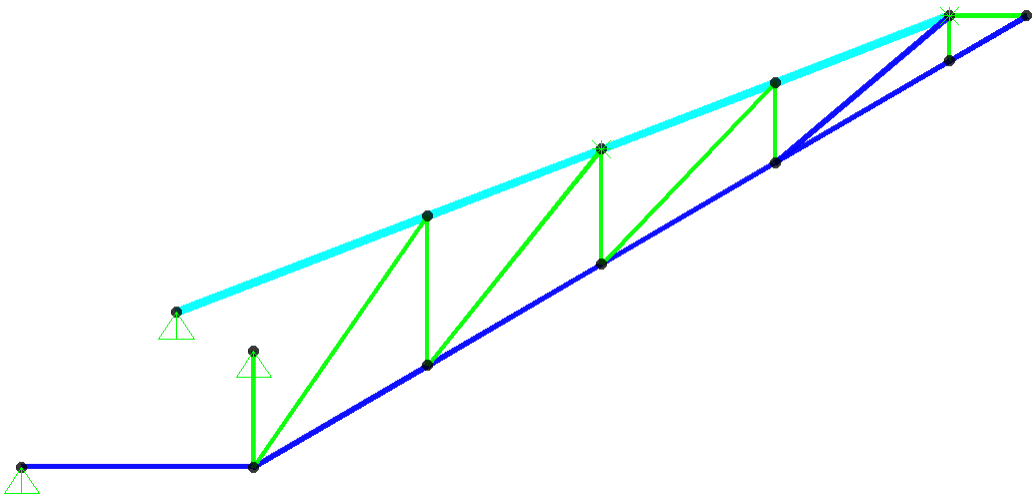

Figure 6.15 : Support's view of the truss on computer software.

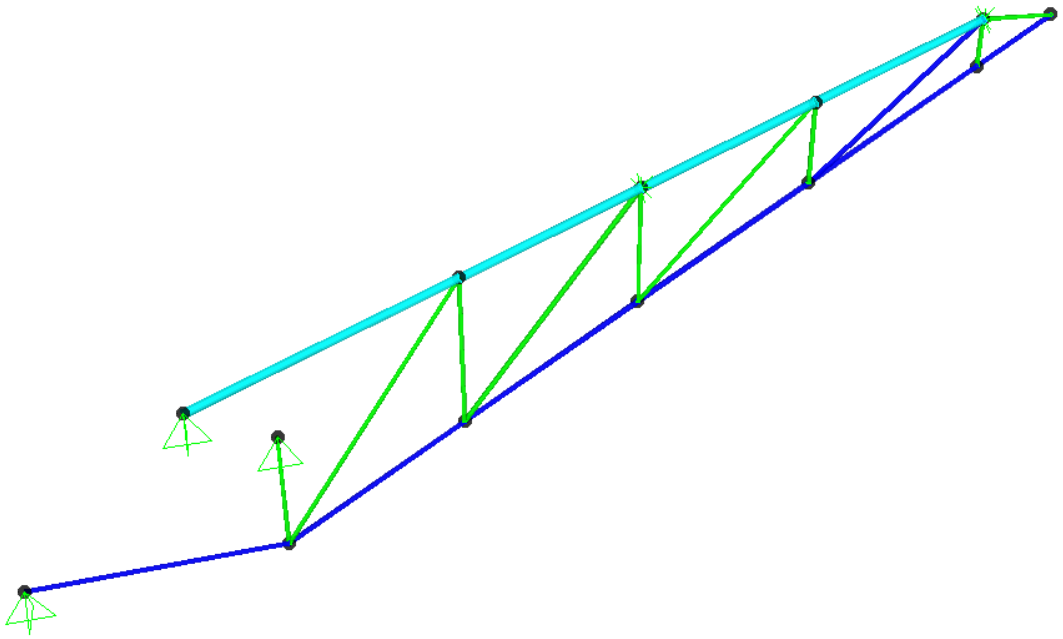

Figure 6.16 : Support's view of the truss on computer software.

6.3 Load Cases

All load cases have been shown in part of system loading shapes.

Table 6.1 : Force which is occurred in 2^{o} degree of angle of attack.

Load Pattern Definitions		
Load Pat	DesignType	Self Weight Multiple
Text	Text	Unitless
DEAD	DEAD	1
G	DEAD	0
LIFT	WIND	0
DRAG(-)	WIND	0
DRAG(+)	WIND	0
Moment	WIND	0

6.3.1 Dead load (G)

For all weight analysis following acceptances have been used.
Steel weight per unit of volume γ=78.5 kN/m³

- Dead load (system's self weight) is added to the analysis automaticaly by SAP2000 software.

6.3.2 The weight of the wing (G)

The weight of the wing: 1236,2 kg : 12,12 kN from ANSYS design.

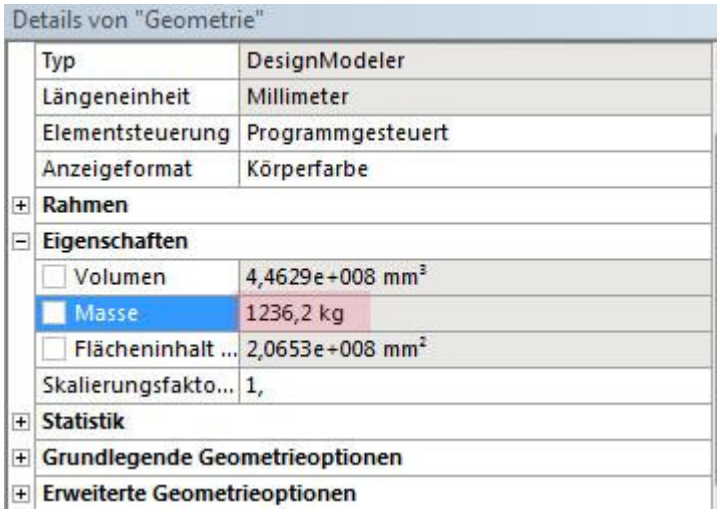

Figure 6.17 : The weight of the wing.

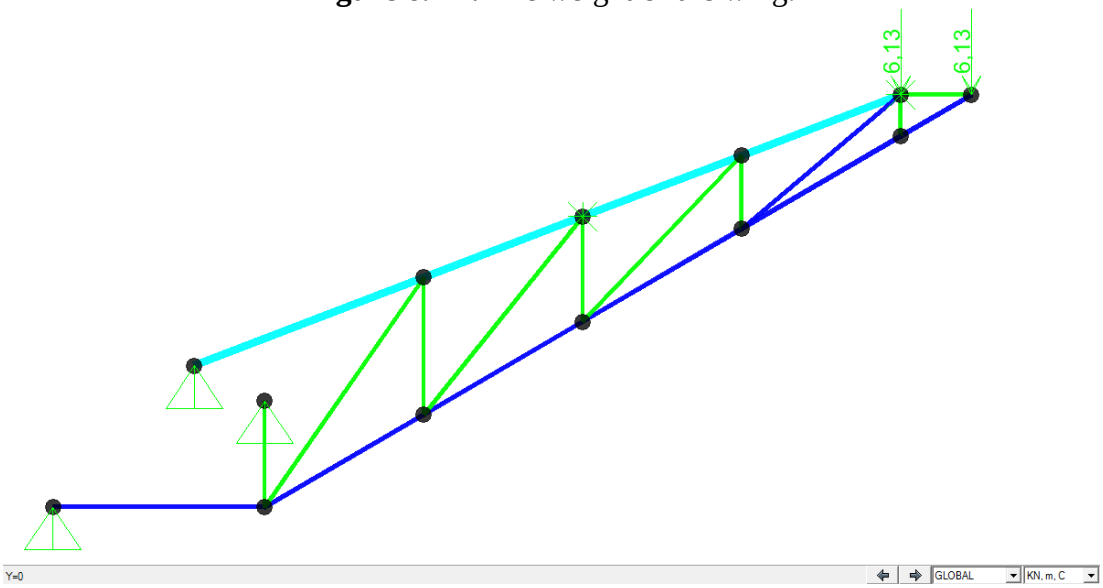

Figure 6.18: 6,13 kN the weight of the wing for two support point.

6.3.3 Wind loads; lift, drag and moments

Wind loads have been obtained from restrained reactions of wind design on ANYSY model.

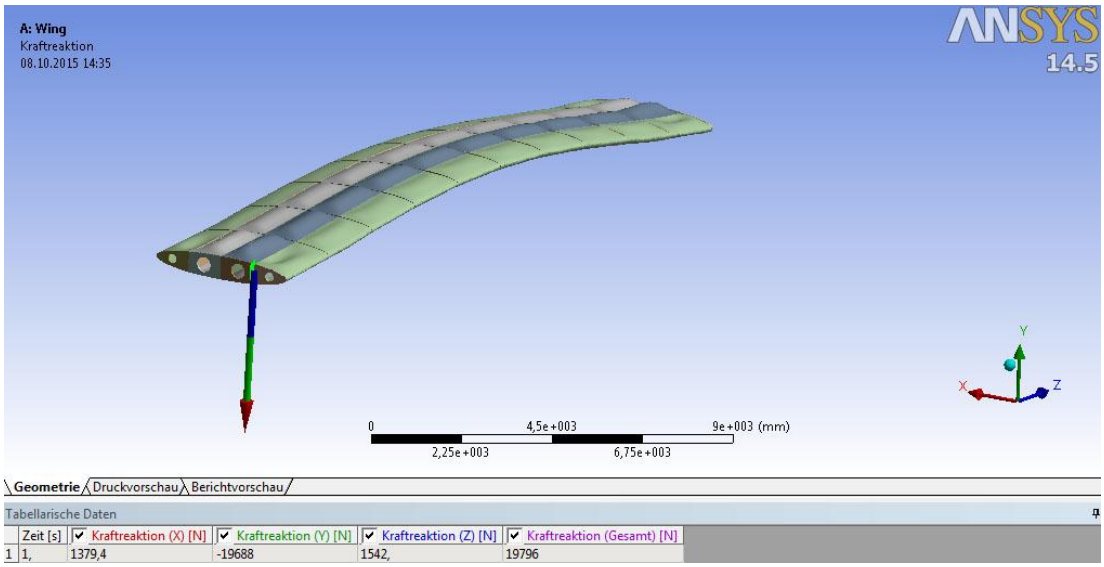

Figure 6.19: 6,13 kN the weight of the wing for two support point.

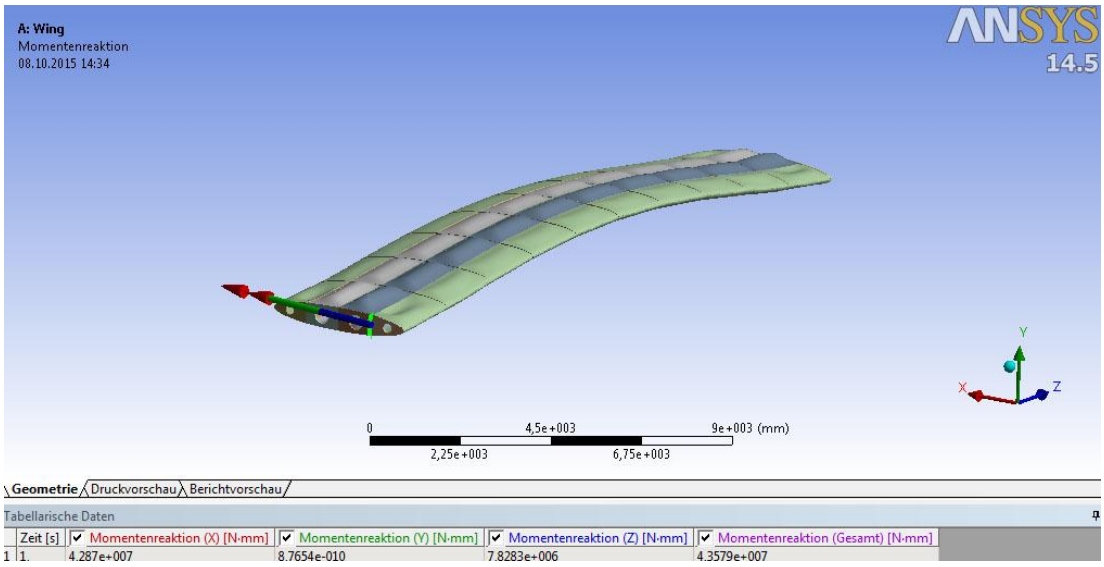

Figure 6.20: 7,82kNm total moment under the total wind forces

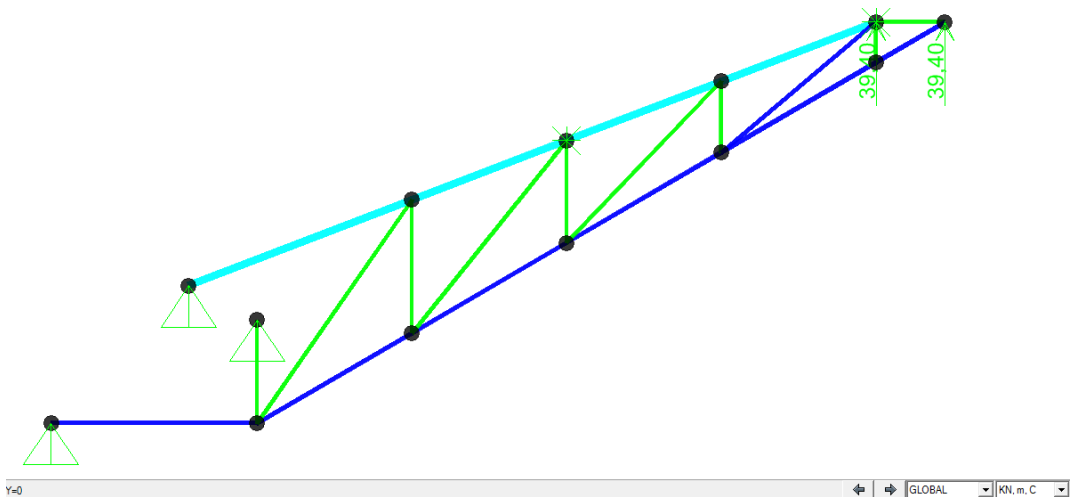

Figure 6.21: 39,40 kN the lift force obtained from the wing for two support points.

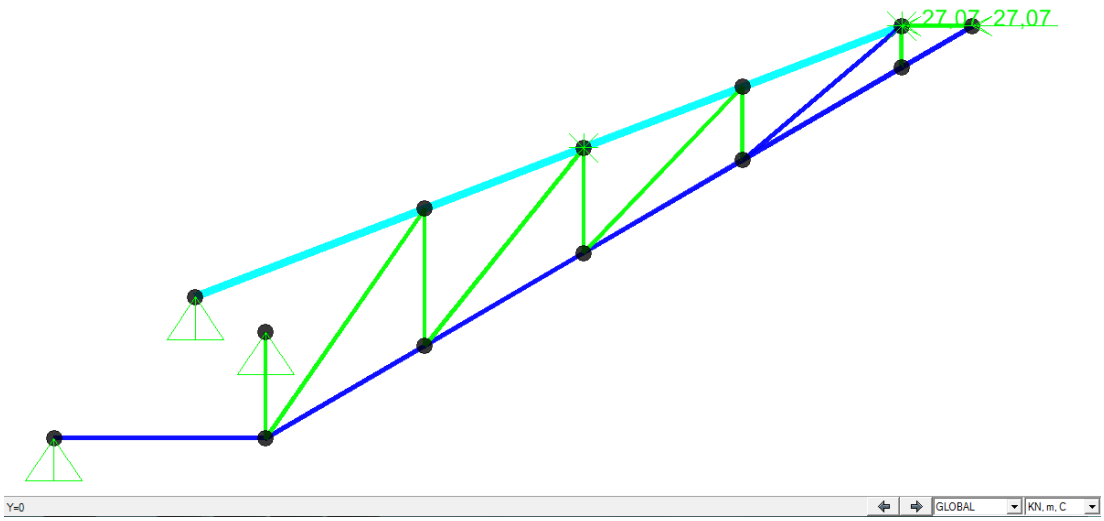

Figure 6.22 : 27,07 kN the drag force obtained from two support points of the wing.

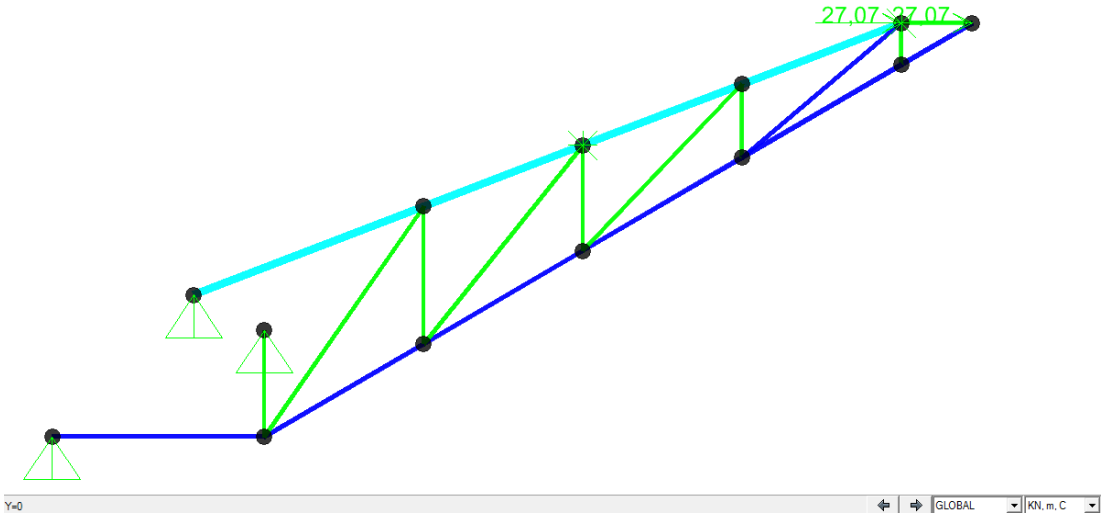

Figure 6.23: 27,07 kN the drag force obtained from two support points of the wing in the opposite direction

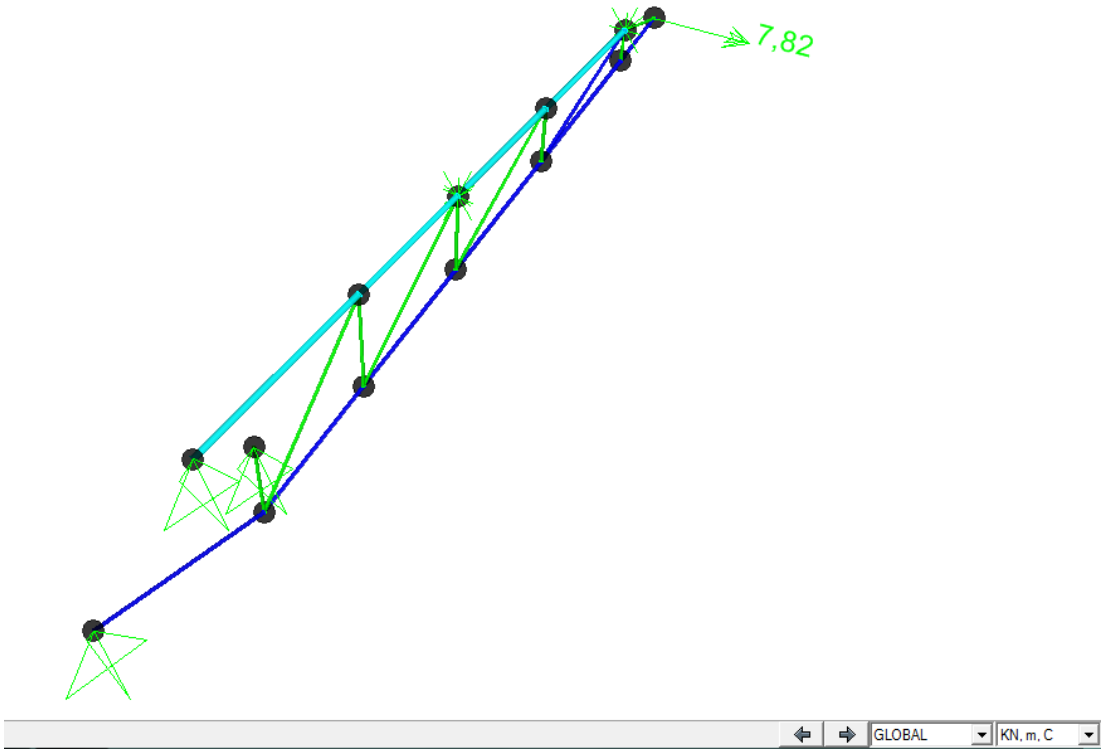

Figure 6.24 : 7,82 kN used to calculate the moment which is obtained from two support points of the wing.

6.3.4 Load combinations

6.3.5 Eurocode load combinations

According to Eurocode 3 combination coefficients γ and Ψ_0 are given below.

Table 6.2: Combination coefficients.

Combination coefficient	Load Type	Value
γ_G	Dead Load (DEAD, DL)	1,35
γ_{Q1}	Wind Load	1,50
Ψ_{0i}	Snow Load (S)	0,50
	Live Load (LL)	0,70

Table 6.3: Force which is occurred in 2^{o} degree of angle of attack.

Combination Definitions					
ComboName	Combo Type	Auto Design	Case Type	Case Name	Scale Factor
Text	Text	Yes/No	Text	Text	Unitless
1,35G+1,50L+1.5D+1.5M	Linear Add	No	Linear Static	DEAD	1,35
1,35G+1,50L+1.5D+1.5M			Linear Static	G	1,35
1,35G+1,50L+1.5D+1.5M			Linear Static	LIFT	1,5
1,35G+1,50L+1.5+1.5M			Linear Static	DRAG(-)	1,5
1,35G+1,50L+1.5D+1.5M			Linear Static	Moment	1,5
1,00G+1,50L+1,5D+1,5M	Linear Add	No	Linear Static	DEAD	1
1,00G+1,50L+1,5D+1,5M			Linear Static	G	1
1,00G+1,50L+1,5D+1,5M			Linear Static	LIFT	1,5
1,00G+1,50L+1,5D+1,5M			Linear Static	Moment	1,5
1,00G+1,50L+1,5D+1,5M			Linear Static	DRAG(-)	1,5

G: Gravity and Dead Load, D: Drag Load, L: Lift Load, M: Moment Load

6.3.6 Steel structural system's elements capacity checks

Structural design has been carried out according to Eurocaode 3-1993 which has been already assigned in software itself.

Table 6.4: Design specification.

EN 1993-1-1:2005	Eurocode 3: Design of steel structures - Part 1-1: General rules and rules for buildings

Table 6.5: Material properties as per Eurocode 3

Steel	Nominal thickness of the element, t (mm)			
	t ≤ 40 mm		40 mm ≤ t ≤ 80 mm	
	f_y (N/mm^2) Yield Stress	f_u (N/mm^2) Ultimate Stress	f_y (N/mm^2)	f_u (N/mm^2)
EN 20025-2				
S235	235	360	215	360
S275	275	430	255	410
EN 20025-3				
S275 N/NL	275	390	255	370
EN 20025-4				
S275 M/ML	275	370	255	360
EN 20025-5				
S235 W	235	360	215	340

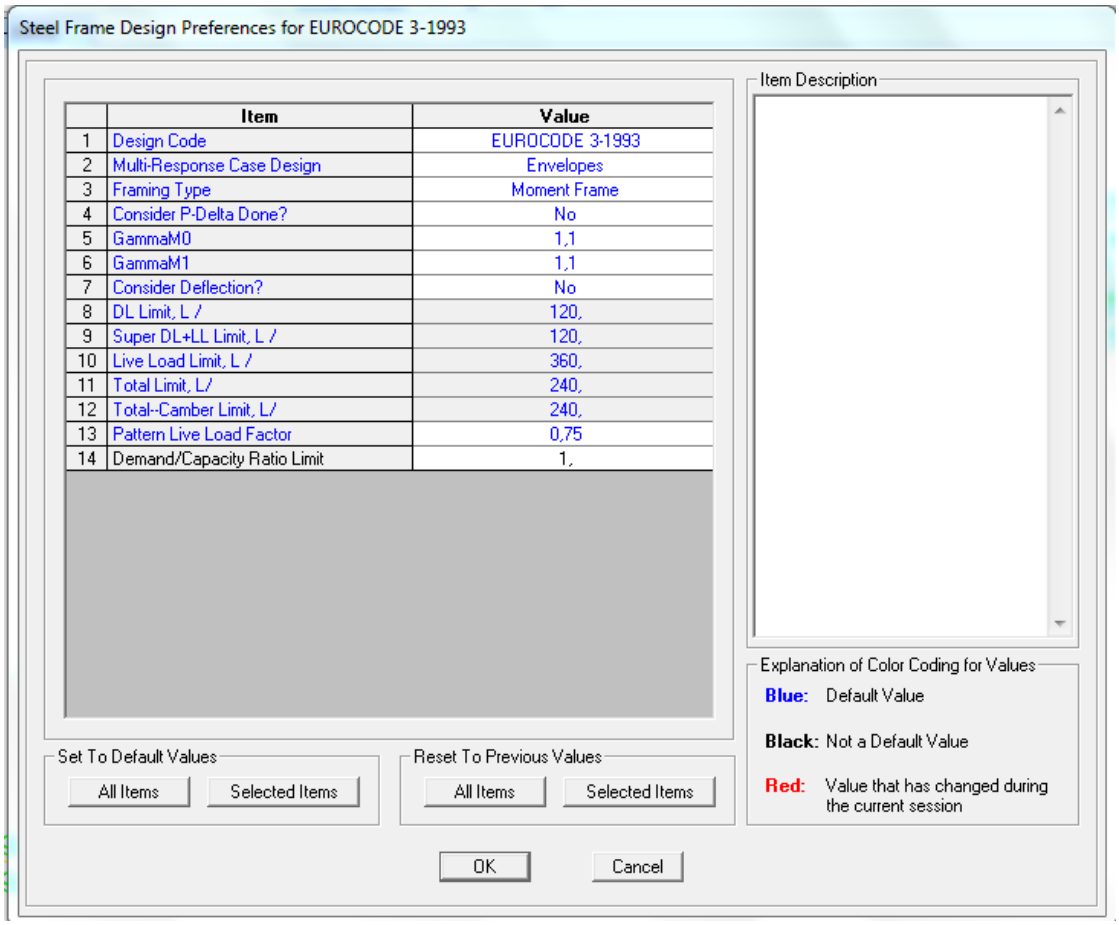

Figure 6.25 : 6,13 kN obtained for the weight of the wing on two support points.

6.3.7 Capacity ratios

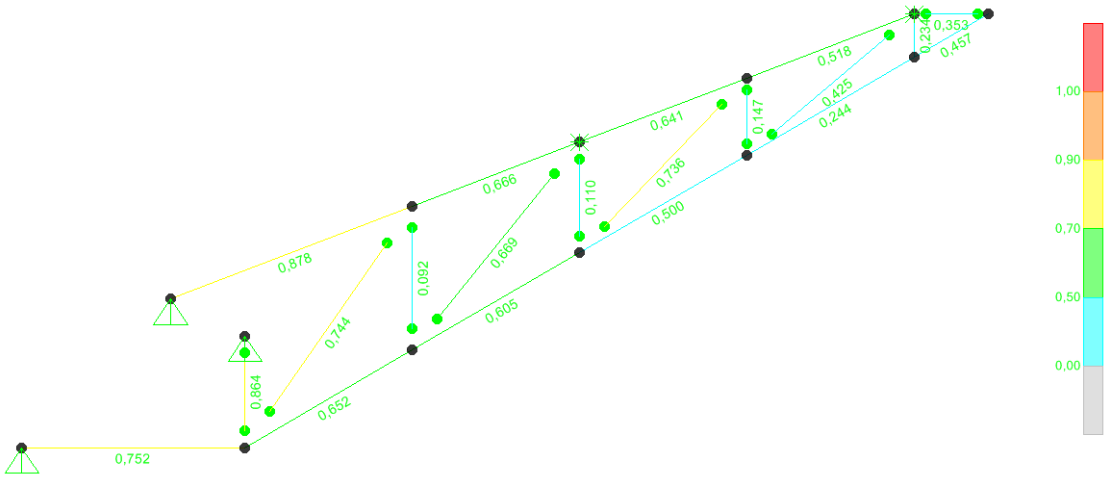

Figure 6.26: Ratio view.

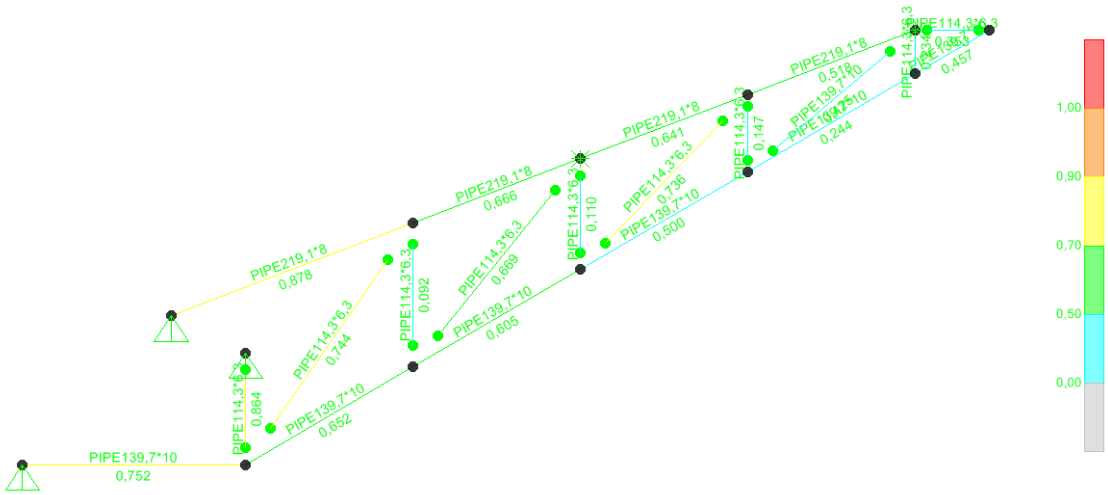

Figure 6.27: Ratio view and pipe sections

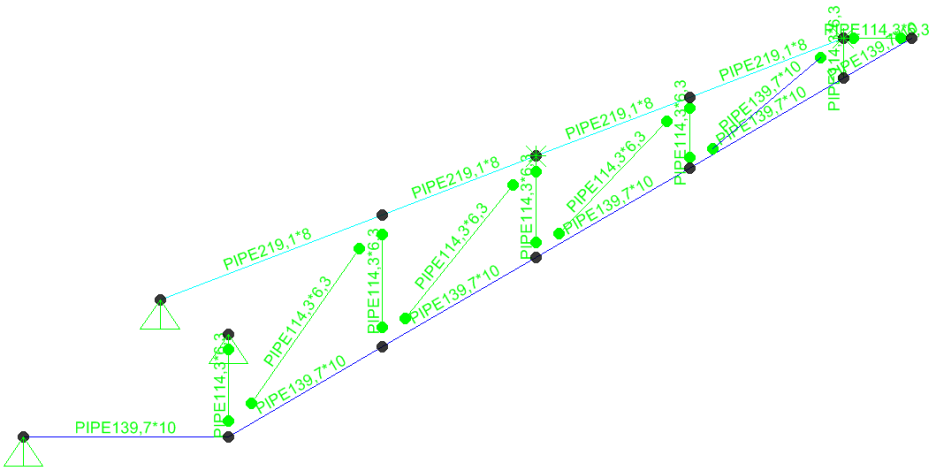

Figure 6.28: Pipe sections

6.3.8 Support analsys results

Table 6.6: Material List 1 - By Object Type from Sap2000

Material List 1 - By Object Type			
ObjectType	Material	TotalWeight	NumPieces
Text	Text	Ton	Unitless
Frame	S235JR	2,6264	20

Table 6.7: Material List 2 - By Section Property from Sap2000

Material List 2 - By Section Property				
Section	ObjectType	NumPieces	TotalLength	TotalWeight
Text	Text	Unitless	m	Tonf
PIPE219,1*8	Frame	4	21,41314	0,8917
PIPE139,7*10	Frame	7	35,02664	1,1202
PIPE114,3*6,3	Frame	9	36,62468	0,6145

6.4 Wing, Support and Bridge Deck Configuration

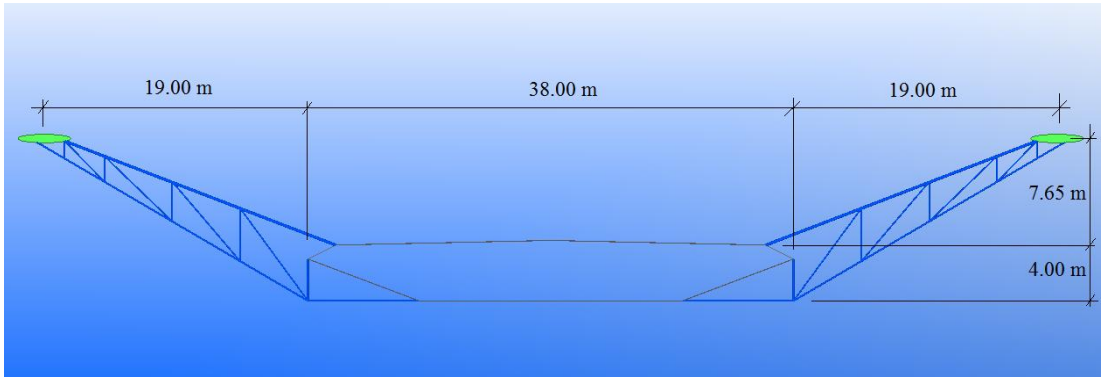

Figure 6.29: Wing, support and deck configuration

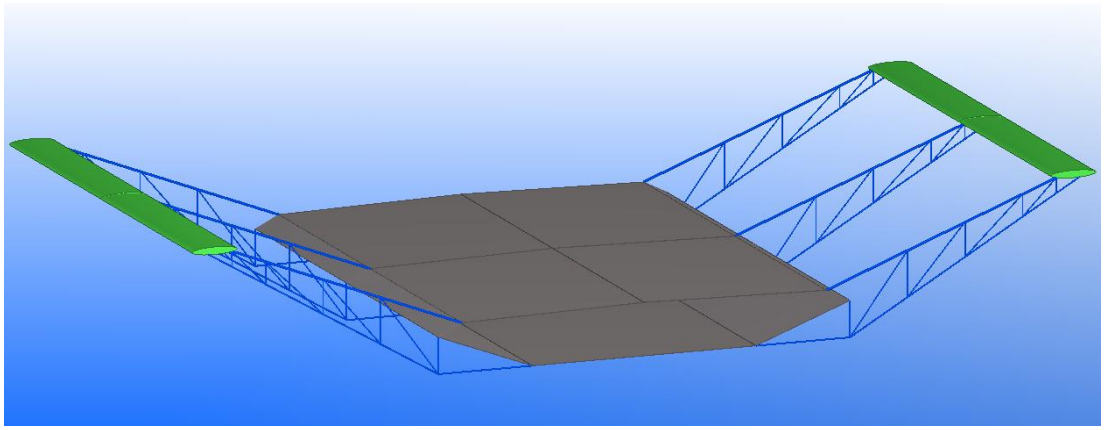

Figure 6.30: Wing, support and deck configuration view

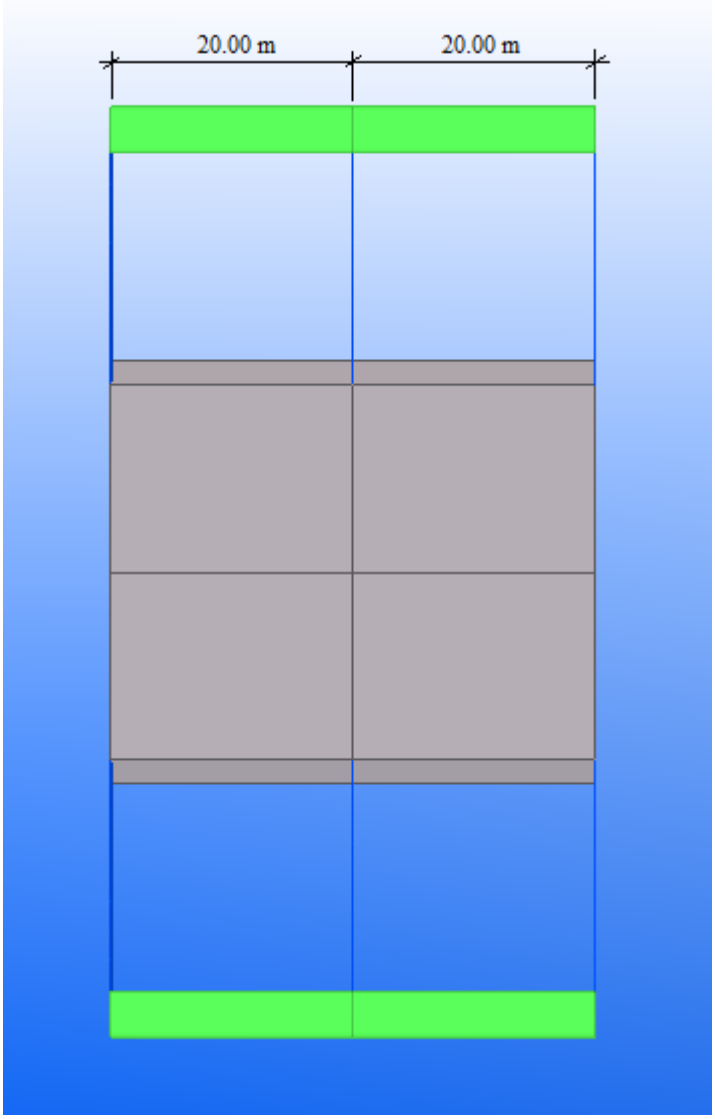

Figure 6.31: Plan view of wing, support and deck configuration for 2 deck section.

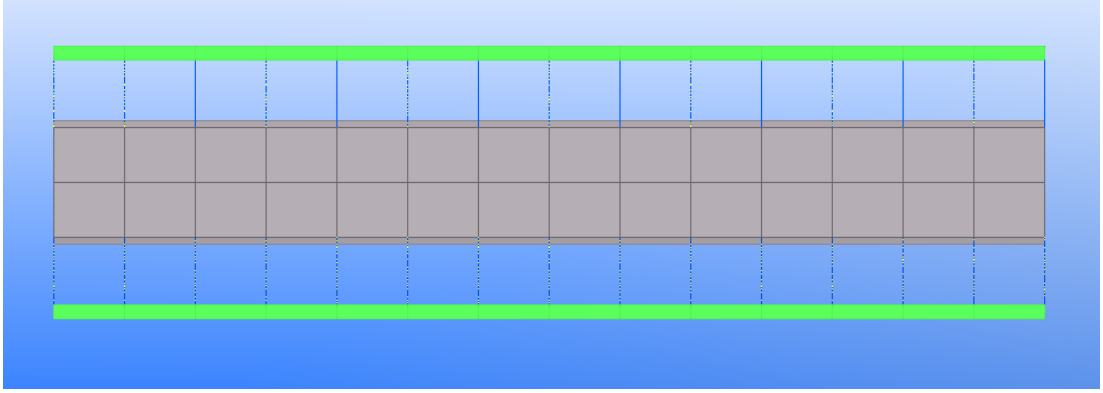

Figure 6.32: Plan view of wing, support and deck configuration plan view for several sections.

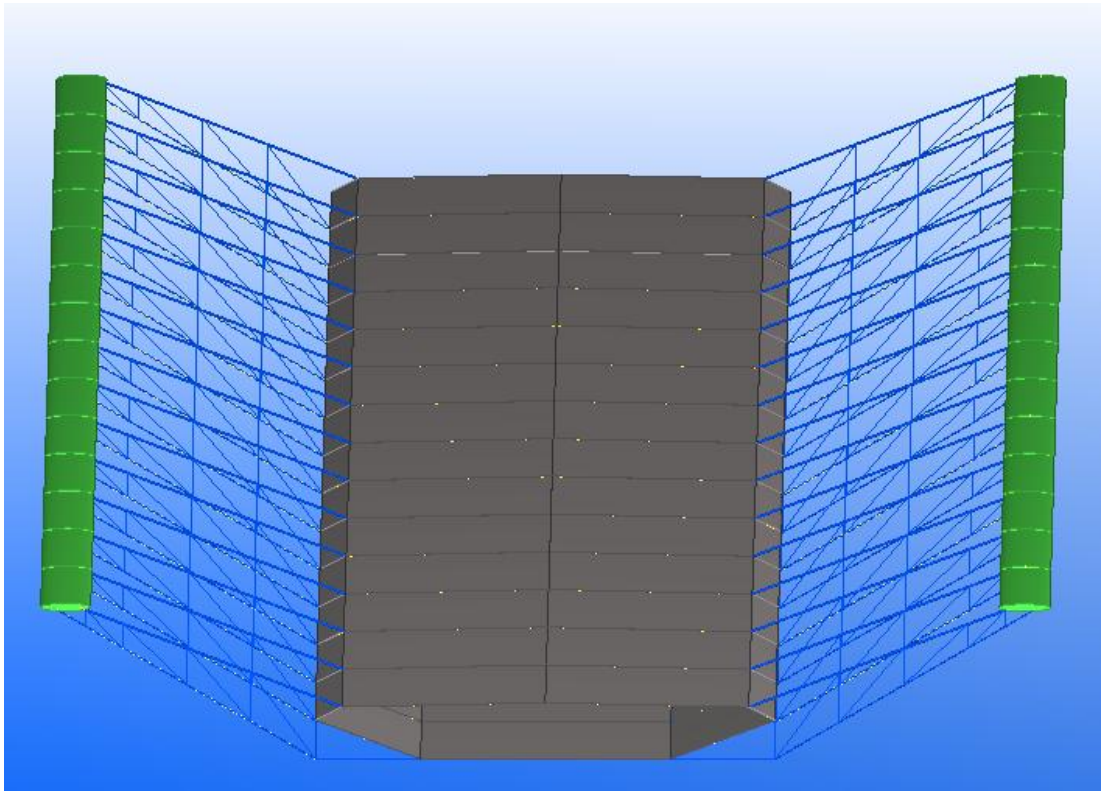

Figure 6.33: 3D view of wing, support and deck configuration.

7. CONCLUSIONS AND RECOMMENDATIONS

The stress analyses of the wing has been carried out by using ANSYS software which is based on Finite Element Methods in this part. In this scope, the wing structure was built in order to raise the critical wind speed from 46,3m/sn to 59,3m/sn by means of a wing structure of the flutter resistance bridges. It was conducted a numerical study for a fictitious system by means of finite element method.The influence of the wing has been identified generally favorable. By considering the cost efficiency, it can be said that the weight of the wing 1235 kg is sufficient for this study of the relevant subject

Further investigations can devote themselves to traditional systems again but not only considering the weigth of the wing but also the wight if the support. The distance between supports can be increased and the weight can be decreased in this way.

The weight of the truss support structure has been observed as 2500 kg per support. Support’s material has been choosen as steel in order to design the welding assemblies or to connections to deck easier. In the coming studies, supports can be designed by using aluminium by overcoming the connection problem.

REFERENCES

[1] **Wai-Fah Chen** (2011). (2008). Bridge Engineering Handbook, CRC Press, the United States of America.

[2] **You-Lin Xu.** (2013). Wind Effects on Cable-Supported Bridges, Wiley.

[3] **Jan R. Wright, Jonathan E. Cooper** (2015). Introduction to Aircraft Aeroelasticityand Loads, UK.

[4] **M. Sajad Mohammadi (**2013). Wind Loads on Bridges, Analysis of a three span bridge based on theoretical methods and Eurocode 1, Stockholm, Sweden.

[5] **Scanlan, R. H., (**1981). State-of-the-Art Methods for Calculating Flutter, Vortex-Induced, and Buffeting Response of Bridge Structures, Report No. FHWA/RD-80/050, Washington, D.C..

[6] **Berreby, D., (**1992). The great bridge controversy, Discover, Feb., 26–33.

[7] **Cai, C. S.,** (1993) Prediction of Long-Span Bridge Response to Turbulent Wind, Ph.D. dissertation, University of Maryland, College Park.

[8] **Jan R.** Wright, Jonathan E. Cooper (2015). Introduction to Aircraft Aeroelasticity and Loads, UK.

[9] **Simiu, E. and Scanlan, R. H.,** (1986) Wind Effects on Structures, John Wiley & Sons, 2nd ed., New York.

[10] **Stathopoulos, Ted, Baniotopoulos, Charalambos C.**, (2007) Wind Effects on Buildings and Design of Wind-Sensetive Structures, Italy.

[11] **Eurocode 3: Design Of Steel Structures** (2005). European Committee For Standardization, Brussels.

CURRICULUM VITAE

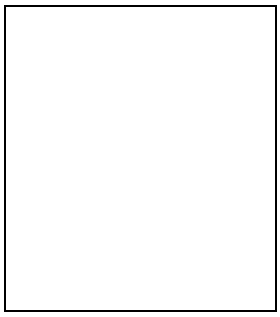

Name Surname: Ibrahim KARLIDAG

Place and Date of Birth: TRABZON-1989

E-Mail: ibrahimkarlidag@gmail.com

EDUCATION:

B.Sc.: Karadeniz Teknik Üniversitesi

PROFESSIONAL EXPERIENCE AND REWARDS:

Karadeniz Teknik University Civil Engineering Department (2011) 3.Place

Design and Construct 2010 Steel Bridge Competition, 1. Place

Prosteel 2011 Steel Structure Design Student Competition (Indoor Sports Hall Contest), Encouragement Award